Chapter 19
NSR–SCR Combined Systems: Production and Use of Ammonia

Fabien Can, Xavier Courtois and Daniel Duprez

19.1 Introduction

Beside the NH_3/urea SCR process, the NOx reduction from lean burn exhaust gas can be achieved using the cycled NOx-Storage Reduction or NSR system (also called Lean NOx-trap (LNT) system). In Europe, the NH_3–SCR technology could be quickly implemented on heavier cars, as it is already the case for trucks, while the NSR system is rather envisaged to be implemented in light passenger car.

However, ammonia may be produced during the regeneration step of NSR catalyst, by the direct reaction (NOx + H_2) or/and the isocyanate route. Ammonia emission is proscribed but this undesirable product is also a very efficient NOx reductant, available in the exhaust gas. Then, logically, the addition of a NH_3–SCR catalyst to the NSR catalyst was proposed in order to increase the global NOx abatement and the N_2 selectivity. Ammonia is produced during the brief regeneration period of the NSR catalyst, and it has to be firstly stored on the SCR catalytic bed. During the next lean period, this stored NH_3 can react with NOx passing through the NOx-trap, via the NH_3–SCR reaction.

Then, the addition of a NH_3–SCR material to the NSR catalyst is a possible way to increase the global NOx abatement and maximize the N_2 selectivity, together with the prevention of the ammonia slip. A schematic view of the process is presented in Fig. 19.1.

This work reports firstly recent results about the production of ammonia during the NSR process, and then an overview of the recent advances in NOx abatement in excess of oxygen using the NOx storage-reduction (NSR)—Selective Catalytic Reduction (SCR) combined systems. With this aim, zeolites are the main studied SCR materials. In addition, studies about the NH_3 storage and the mechanism in NOx reduction over zeolite are presented.

F. Can (✉) · X. Courtois · D. Duprez
UMR 7285, IC2MP, Université de Poitiers, CNRS, 4 rue Michel Brunet,
86022 Poitiers Cedex, France
e-mail: fabien.can@univ-poitiers.fr

I. Nova and E. Tronconi (eds.), *Urea-SCR Technology for deNOx After Treatment of Diesel Exhausts*, Fundamental and Applied Catalysis,
DOI: 10.1007/978-1-4899-8071-7_19, © Springer Science+Business Media New York 2014

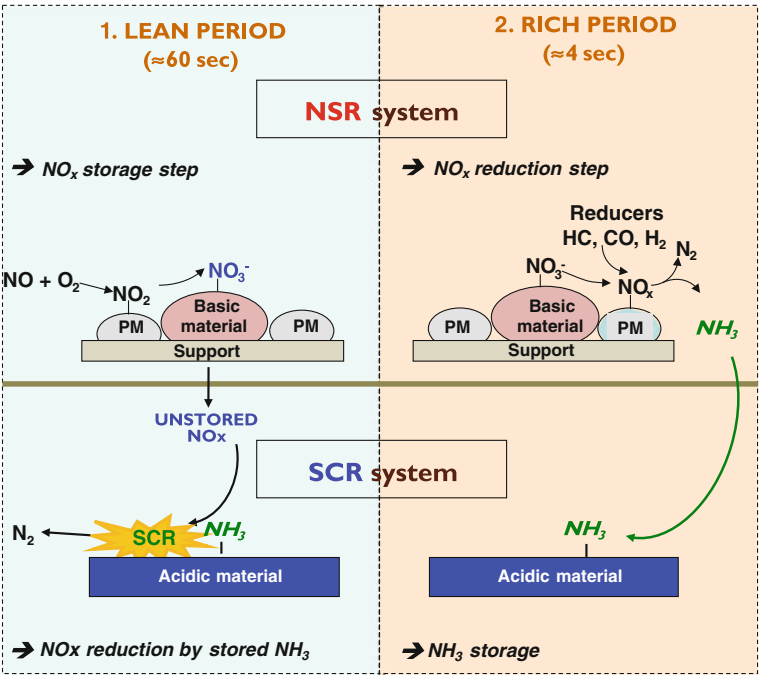

Fig. 19.1 Schematic view of the NSR + SCR combined process

19.2 NH_3 Emission from NSR Catalysts

19.2.1 The NSR Process

The NOx storage-reduction (NSR) process is largely studied since the beginning of the 1990s [1–5]. Model NOx-trap catalysts usually contain a noble metal (Pt) allowing the NO oxidation into NO_2, and a basic phase (Ba oxide/carbonate) in order to trap NO_2 as nitrite/nitrate intermediates. Both precious metals and storage phase are usually supported on a modified alumina support [6]. Other frequent components are rhodium which is known to favor the NOx reduction into N_2 in stoichiometric/rich media, and cerium-based oxides due to their redox behavior, the NOx storage capacity and the sulfur resistance [7, 8]. Among other possible basic storage phases, potassium is the more frequently proposed [9, 10].

The NSR catalyst operates in fast lean/rich transients. During the lean steps of approximately 1 min, the gas phase is constituted by the standard exhaust gas from the lean burn engine. NO is then oxidized into NO_2 over the precious metals and further trapped as nitrite/nitrate on the basic components of the catalyst. The "saturated" trap is then regenerated during short incursions in rich media for few seconds in order to reduce the stored NOx into N_2. In fact, the rich phases are

generated by injecting pulses of fuel, immediately transformed into HC, CO and H_2 on a pre-catalyst (usually a Diesel Oxidation Catalyst implemented before the NSR system). These rich pulses induce exothermic reactions which favor the nitrate desorption and reduction into nitrogen. These steps correspond to the ideal operating mode of the NSR system.

The nature of the reductants in the rich mixture directly impacts the NOx conversion and the selectivity of the NSR reaction. On usual NSR model catalysts, namely $Pt/(BaO)/Al_2O_3$, hydrogen is reported to be the more efficient agent compared with CO or propene [11–13]. This higher efficiency of H_2 was evidenced by Szailer et al. [11] at very low temperature (150), and in the 150–350 °C temperature range by Nova et al. [12]. Nevertheless, undesirable by-products can also be emitted during the regeneration, such as N_2O and ammonia. As an introduction to the NSR + SCR combined system, the following section focuses on the ammonia formation and emission over NSR catalysts.

19.2.2 Ammonia Formation Pathways

Ammonia is reported to be produced only during the rich phases of the NSR process, even in the presence of usual reductant(s) such as H_2, CO or propene during the lean phases [14, 15]. However, note that significant ammonia emission can be observed during the NOx reduction in lean condition using ethanol as reductant [16].

During the regeneration of the NOx trap, two major routes are commonly admitted for the ammonia formation. The first one is the direct reaction of stored NOx with hydrogen, as described in reaction (19.1) [13, 17]. This route was proposed over $Pt–Ba/Al_2O_3$ material, when H_2 is used as the reductant [18]. Artioli et al. [19] observed that, depending on the gas feed composition, ammonia is emitted together with CO_2 consumption, as reported in reaction (19.2).

$$Ba(NO_3)_2 + 8H_2 \rightarrow 2NH_3 + Ba(OH)_2 + 12H_2O \tag{19.1}$$

$$Ba(NO_3)_2 + 8H_2 + CO_2 \rightarrow 2NH_3 + BaCO_3 + 5H_2O \tag{19.2}$$

The catalyst temperature is an important parameter which impacts both the NOx adsorption/desorption equilibrium and reduction rate. Ideally, the NOx reduction rate has to be higher than the NOx desorption rate in order to limit the NOx slip during the rich pulses. During these reduction phases, a part of the introduced reductants also reacts with remaining oxygen from the gas phase or stored on the catalyst. As a consequence, an exothermic phenomenon is generally detected during the rich pulses, which lead to additional releases of unreduced NOx. In fact, it was showed that when the regeneration of the catalyst is carried out in the presence of NO in the feed stream, ammonia can be directly formed according to reaction (19.3) in the reactor zone where the trap is already regenerated [20].

$$NO + 5/2\ H_2 \rightarrow NH_3 + H_2O \quad \text{or} \quad NO_2 + 7/2\ H_2 \rightarrow NH_3 + 2H_2O \quad (19.3)$$

However, it is shown in this work that ammonia is observed after N_2 formation, when hydrogen begins to be emitted. This point is more detailed in Sect. 19.2.3.

The direct ammonia formation mechanism (reactions 19.1 and 19.3), when only H_2 is used as reductant, was studied in Ref. [11]. Authors proposed that hydrogen reacts firstly with the platinum surface on which oxygen species (O_a), resulting from the reduction of NO_2, remain adsorbed (reaction 19.4).

$$Pt^{\cdots}O_a + H_2 \rightarrow Pt* + H_2O \quad Pt* \text{ represents reduced Pt sites.} \quad (19.4)$$

The produced H_2O is supposed to destabilize the adsorbed nitrates which are suggested to be decomposed on the free Pt surface. The dissociation of NOx species on platinum can thereafter leads to the recombination of N_a atoms to form N_2 (reactions 19.5 and 19.6), or to the reaction of these N_a atoms with H_2 to form NH_x and, finally, NH_3.

$$(x + 1)Pt* + NOx \rightarrow xPt^{\cdots}O_a + Pt^{\cdots}N_a \quad (19.5)$$

$$2Pt^{\cdots}N_a \rightarrow 2Pt* + N_2 \quad (19.6)$$

In this step way, the initial role of H_2 is the reduction of the platinum surface to allow the NOx dissociative adsorption [21].

Clayton et al. [22] also suggested that the ammonia formation mechanism includes the activation of H_2 on Pt sites. They proposed that adsorbed nitrates are decomposed into NOx and released in the gas phase, due to hydrogen spill-over from the noble metal to the alumina support. NOx species are readily reduced to ammonia due to high local H/N ratio.

The second way to obtain ammonia during the NSR regeneration is the "isocyanate route" [23]. This intermediate reaction is observed when a carbon source is present in the reaction mixture, especially CO [11]. However, CO can also be produced in situ, for instance by the reverse water gas shift (RWGS) reaction between H_2 and CO_2, the later being always present in large amounts in a real exhaust gas (see also the influence of the WGS equilibrium Sect. 19.2.3).

At low temperature ($T < 150$ °C), the first reaction is still the removal of adsorbed oxygen atoms from the Pt particles ($Pt^{\cdots}O_a$), leading to CO_2 production (reaction 19.7).

$$Pt...O_a + CO \rightarrow Pt* + CO_2 \quad (19.7)$$

The obtained free Pt sites become available for the NOx dissociative adsorption and the CO adsorption. Then, formation of adsorbed NCO species is possible according to reaction 19.8.

$$Pt...N_a + Pt...CO_a \rightarrow Pt* + Pt{-}NCO_a \quad (19.8)$$

−NCO species generated on the Pt particles migrate to the oxide components of the catalyst, usually alumina. Therefore, −NCO and CO_2 formation occur at the expense of the reduction of the adsorbed NOx, while N_2 is not produced.

At higher temperatures ($T > 300$ °C) these −NCO species are able to react with the stored NOx. This reaction route eventually leads to the consumption of both nitrate and NCO adsorbed species according reaction 19.9.

$$NCO_a + NOx \rightarrow N_2 + CO_2 \tag{19.9}$$

In real exhaust gas, water is present with a large extent and it is reported that N_2 formation is significantly enhanced by adding water to the NCO-covered catalysts [10]. Adding water leads to a new reaction route for the −NCO reactivity, i.e., the hydrolysis of −NCO species to NH_3 and CO_2 (reactions 19.10 and 19.11).

$$NCO_a + H_2O \rightarrow NH_{2/a} + CO_2 \tag{19.10}$$

$$NH_{2/a} + H_2O \rightarrow NH_3 + OH_a \tag{19.11}$$

To conclude, ammonia can be formed only during the regeneration steps of the NOx-trap, even if ammonia release can also occur during the subsequent lean phase. Two pathways are described: the direct reaction of H_2 with the stored NOx or with NOx present in the gas phase, and via the hydrolysis of isocyanates species. Hydrogen is reported as a more efficient reductant than CO, leading to a higher emission of ammonia [11, 12].

19.2.3 Influencing Parameters/Ammonia Reactivity

Numerous parameters were studied and reported as influencing the ammonia emissions from the NSR catalyst.

Dispersions of the catalyst components were reported to strongly modify the NH_3 emission, For instance, Castoldi et al. have observed that ammonia emission occurs during the NOx-trap regeneration when barium loading ranges from 16 to 30 wt. % [18]. At lower barium loading (i.e., 5–16 wt. %), authors have reported that the reduction of stored NOx is initially fully selective into nitrogen.

Bhatia et al. [24] have modeled the effect of the platinum dispersion of a model $Pt/BaO/Al_2O_3$ sample, also taking into account the influence of the temperature. This study indicates that at high temperature ($T \geq 300$ °C), highest amounts of NH_3 are produced over low dispersed catalyst (3.2 % platinum dispersion). On the contrary, it was observed that ammonia formation is enhanced at low temperature ($T \leq 200$ °C) with the highly dispersed catalyst (50 % dispersion) [24]. The effect of noble metal dispersion on ammonia production is explained by the variation of the average distance—or proximity—between the stored NOx and the platinum sites. Proximity between storage sites and reaction sites is known to affect the stored NOx transport process [25].

As presented in Sect. 19.2.2, two main routes are proposed to produce N_2 when H_2 is the reductant: (i) the direct route, from the reduction of stored NOx by H_2 and (ii) the sequential route through NH_3 intermediate formation [22, 26], which can be simply described following reactions (19.12–19.13).

$$H_2 + NOx \rightarrow NH_3(\text{step 1}) \tag{19.12}$$

$$NH_3 + NOx \rightarrow N_2(\text{step 2}) \tag{19.13}$$

This two-step mechanism was evidenced in Refs. [27] and [34] over a model Pt–Ba/Al_2O_3 catalyst. As a consequence, when the amount of introduced hydrogen is too low to reduce all the stored NOx, incomplete regeneration of the catalyst is observed. Such an incomplete regeneration obviously results in a decrease of the storage capacity for the subsequent lean periods. Beside, the reaction of the stored NOx with hydrogen results in the formation of negligible amounts of N_2O and NH_3, nitrogen being the only product detected at the reactor exit. It induces that no ammonia is observed as long as hydrogen is fully consumed. It is especially true for temperature higher than 300 °C, as confirmed by different works [12, 28, 29].

In opposition, the NOx reduction selectivity is strongly affected by ammonia emission since hydrogen is not fully converted during the pulses. In Table 19.1 are reported some results from the literature in which the hydrogen concentration measurement at the reactor outlet is available. Table 19.1 shows that, whatever the NOx conversion rate, ammonia is released when hydrogen is not fully consumed during the regeneration step of the NOx-trap catalyst.

An illustration of these observations is shown in Fig. 19.2. This figure reports the influence of the catalytic mass and the hydrogen concentration in the rich pulses at 400 °C. It allows following the evolution of the reactions along the catalytic bed. The increase of the catalytic weight clearly shows that the in situ produced ammonia during the NOx reduction on the first part of the catalyst is able to react with the downstream stored NOx to give N_2 since there is no more available hydrogen [28]. On the contrary, if hydrogen remains, all the catalytic bed works identically.

In agreement with Nova et al. [31], this Fig. 19.2 also strongly suggests that (i) nitrogen formation occurs via a two step pathway and (ii) the stored NOx react preferentially with the introduced hydrogen to form NH_3 (step 1), whenever H_2 is present in the gas phase. NH_3 further reacts with stored NOx downstream to form N_2, preferentially in a hydrogen free environment (step 2) [28, 34]. The selectivity toward NH_3 formation is then governed by the relative rate constants of NH_3 formation and NH_3 consumption. In this dual-step mechanism, step 1 rate is higher than the step 2 one [17, 32], even though the characteristic reaction times for NH_3 formation and consumption are lower than the characteristic diffusion times of stored NOx.

As previously mentioned, the presence of H_2O and CO_2 in the gas mixture directly impacts ammonia formation mechanism. According to reaction (19.14), the Water Gas Shift (WGS) and the reverse reaction (Reverse WGS, RWGS) can

Table 19.1 Examples of data from the literature about the correlation between the ammonia emission and the presence of unconverted hydrogen during storage/reduction cycled experiments

Ref.	Lietti et al. [32]	Pereda–Ayo et al. [27]	Castoldi et al. [18]	Bhatia et al. [24]	Kočí et al. [13]	Nova et al. [12]	Artioli et al. [19]	Choi et al. [30]
Catalyst	Pt–Ba/Al	Pt–Ba/Al monolith	Pt–Ba/Al	Pt–Ba/Al	Industrial	Pt–Ba/Al	Pt–Ba/Al	Industrial
T (°C)	100	260	350	370	250	200	350	200
H_2 inlet	2000 ppm	0.85 %	2000 ppm	1500 ppm	3.3 %	2000 ppm	4000 ppm	3.4 %
H_2 outlet	80 ppm	Traces	600–150 ppm	700 ppm	0.5 %	300 ppm	1000 ppm	1.4 %
NH_3 outlet	400 ppm	300 ppm	150–400 ppm	330 ppm	2200 ppm	180 ppm	500 ppm	120 ppm

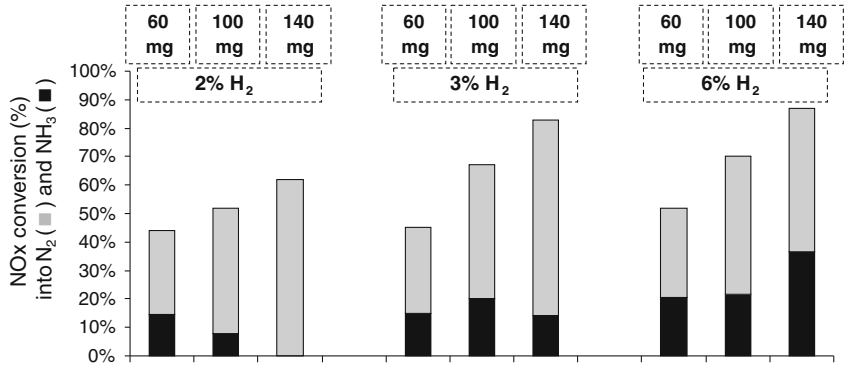

Temp.	400 °C	400 °C	400 °C	400 °C	400 °C	400 °C	400 °C	400 °C	400 °C
H_2 conv.	88%	99%	100%	85%	95%	99%	63%	79%	79%
N_2 selec.	67%	85%	100%	67%	70%	83%	57%	69%	58%
NH_3 selec.	33%	15%	0%	33%	30%	17%	43%	31%	42%
NOx conv.	44%	52%	62%	45%	67%	83%	48%	70%	87%

Fig. 19.2 Pt/Ba/Al_2O_3 catalyst: NOx conversion at 400 °C under cycling lean (60 s, 500 ppm NO, 10 % O_2, 10 % H_2O, 10 % CO_2)/rich (3 s, H_2, 10 % H_2O, 10 % CO_2) condition. NOx conversion (%) into N_2 ( ) and into NH_3 ( ) and related data. Influence of both the H_2 concentration in the rich pulses (1–6 %) and the catalyst mass (60, 100, and 140 mg), from [28]

also occur, leading to the presence of both CO and H_2 in gas phase, even if the initial reductant in the rich mixture is H_2 or CO alone.

$$CO + H_2O \rightleftharpoons CO_2 + H_2 \tag{19.14}$$

It was demonstrated that the presence of water or carbon dioxide in the gas mixture has a negative effect on the storage step of the NSR process [33, 34]. However, their impacts on the reduction step using H_2 as reductant are significantly different. Due to the involvement of water in the (R)WGS reaction, the absence of few percents of H_2O in the gas mixture leads to a small decrease of the NOx removal efficiency because a larger part of the introduced hydrogen is transformed into CO, a less efficient reductant. In the same time, the ammonia selectivity increases due to the possible formation of isocyanate species. In opposition, the absence of CO_2 leads to an increases in NOx conversion [34], with a little ammonia formation. The isocyanate is then impossible since there is no carbon source in the gas mixture. However, ammonia emission can still be observed, indicating that the direct route occurs. Note that hydrocarbons (such as propene) are also possible reductants leading to isocyanates via oximes intermediates [35]. Isocyanates lead to amines (or amides) that are very good reductants of NOx [35, 36].

The nature of the basic storage phase also affects the ammonia formation. For instance, the comparison of usual Pt–Ba/Al_2O_3 catalyst with Pt–K/Al_2O_3 sample (with similar molar amount of basic element, i.e., Ba or K) evidences a higher N_2 selectivity during the reduction step with H_2 for the NOx stored over the K phase [17]. Authors report a similar reactivity for the H_2 + nitrate and NH_3 + nitrate

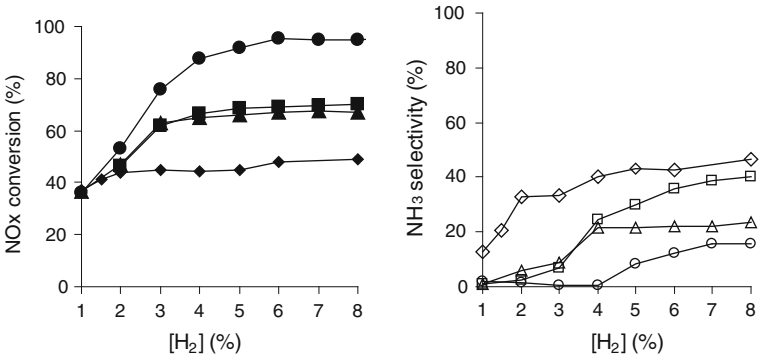

Fig. 19.3 NOx conversion rate (*full symbols*) and NH_3 selectivity (*open symbols*) measured at 400 °C depending on hydrogen concentration in the rich pulses for Pt/20Ba/Al (◆, ◇), Pt/20BaMn/Al (■, □), Pt/20BaCe1/Al (▲, △) and Pt/20BaMnCe0.5/Al (●, ○) [29]

reactions. In fact, on Pt–K/Al_2O_3, the onset for the direct H_2 + nitrate reaction leading to ammonia (step 1, reaction 19.13) occurs at temperature very close to the threshold for the NH_3 + nitrate reaction (step 2, reaction. 19.14), leading to the desired N_2 compound. Finally, this study shows again that the ammonia emission strongly depends on the balance between the ammonia production and the ammonia reaction with the stored NOx.

The nature of the support, especially in terms of redox properties, obviously significantly impacts this equilibrium between formation and reactivity of NH_3 during the regeneration step of the NSR process. It is possible to increase the reaction rate between the in situ produced ammonia and the remaining stored NOx. For instance, addition of manganese to a Pt/BaO/Al_2O_3 model material (Pt/Ba(Mn)/Al catalyst) allows an improvement of the NOx reduction by ammonia, especially at 400 °C, even if the introduced hydrogen is not fully converted [28]. Same trends were obtained with addition of ceria, and more interestingly, further improvements were obtained with the simultaneous Mn and Ce addition to model Pt/BaO/Al_2O_3 catalyst [29]. A synergetic effect was highlighted between Mn and Ce with a significant decrease in ammonia emission in the 200–400 °C temperature range, correlated with a synergetic effect concerning the oxygen storage capacity. The influence of the Mn and Ce addition on the NOx conversion rate and the NH_3 selectivity at 400 °C are presented in Fig. 19.3 depending on hydrogen concentration in the rich pulses. The increase of the NOx conversion together with the decrease of the ammonia selectivity was partially attributed to an enhancement of the reactivity between the in situ produced ammonia and the stored NOx.

In addition to the enhancement of the NOx + NH_3 reaction rate, the selective ammonia oxidation into nitrogen via the available oxygen was also proposed to occur [22]. Then, this reaction was proposed to explain the low NH_3 emission obtained with the catalysts exhibiting high oxygen storage capacities (OSC), even with very large hydrogen excess (Fig. 19.3), [37]. However, the OSC/oxygen mobility is not the only parameter to explain the activity enhancement. It was showed over Pt/$Ce_xZr_{1-x}O_2$

catalysts that the NH_3 yield is decreased with the increase of the cerium content, but not with the OSC [38]. This aspect is not totally explained yet.

19.2.4 Conclusion

Finally, significant ammonia emissions are possible at the NSR catalyst outlet. Two pathways are described, the direct route with H_2 and the isocyanate route with CO. However, the ammonia formation is especially favored in the presence of hydrogen, which can be produced in situ or upstream the NSR catalyst. Whatever the ammonia production pathway, ammonia emission strongly depends on the balance between the ammonia formation rate and the ammonia reactivity (with NOx or oxygen from the support). Ammonia emission is particularly linked to the presence of unconsumed hydrogen. In addition, Ce-based oxides are proved to enhance the ammonia reactivity in the NSR catalyst.

19.3 Coupling of NOx Trap and NH_3–SCR Catalysts

19.3.1 Emergence and Development of the NSR–SCR Coupling Concept

The concept of adding a NH_3 adsorbing materials to a NOx reduction catalyst was patented by Toyota in 1998 for applications on gasoline engines [39]. In the claimed configuration, a Cu–ZSM-5 catalyst is added to the three way catalyst (TWC) with the engine working in cycling conditions. In rich conditions, NOx can be reduced to N_2 and NH_3 which can be stored on the zeolitic materials. When the engine turns to lean conditions, NOx is no longer reduced on the TW catalyst. Ammonia is in part oxidized (to N_2) or desorbed. It may then react with NO passing through the TW monolith. This initial system was improved by introducing a small, auxiliary engine working in rich conditions and able to produce ammonia needed for reduction of the NOx issued from the main engine [40]. Exhaust pipes are arranged to receive a TWC catalyst and a NH_3 adsorbing materials. In a further patent, Toyota claimed a new embodiment of the concept in which a group of cylinders are working in rich conditions while the others are working in lean conditions [41]. TW catalysts and NH_3 adsorbing and oxidizing catalysts (NH_3–AO) are interconnected to receive alternatively the gases issued from the first and second groups of cylinders. The patent claims a wide range of NH_3–AO catalysts: zeolites, silica–alumina, titania doped with Cu, Fe, Cr,… This last system was finally improved by replacing the TW catalyst by a NOx-trap materials (named NOx-occluding and reducing catalyst, NH_3–OR in the patent) [42]. In this configuration, the system is very close to the NSR–SCR coupling for

NOx after-treatment. Several systems associating NSR and SCR catalysts were further claimed in Toyota patents [43, 44].

A system including an ammonia-generating catalyst coupled with the NOx-trap or a TW catalyst was claimed by Daimler–Chrysler in 2002 under the name of "smart catalytic converter" [45]. In the lean operating phases, the nitrogen oxides are intermediately stored in the nitrogen oxide adsorption catalyst. In the rich operating phases, ammonia is generated by the ammonia-generating catalyst from the nitrogen oxides contained in the exhaust gas. The generated ammonia then causes a nitrogen oxide reduction in the nitrogen oxide adsorption catalyst. The mechanism by which ammonia is generated is obviously not detailed. The patent merely supposes that ammonia can be formed by reaction of NOx with reductants in excess (especially H_2) during the rich operating phases. The materials catalyzing the reaction between NO and ammonia are not fully described. It is suggested that the SCR reaction can occur on the NOx adsorbing catalyst. Commercially, the system was implemented on the Mercedes E320 Bluetec vehicle in 2007.

The coupling between a NOx-trap sample and a NH_3–SCR catalyst, located downstream the first one or in a double layer on the monolith, was patented by Ford in 2004 [46]. In this patent application, ammonia is generated during the rich spike of the NSR catalyst cycle. It is stored on the SCR catalyst and further used to reduce NOx during the lean phase. Depending on the temperature, a significant fraction of the nitrogen oxides may not be trapped and passes through the NSR catalyst: the SCR catalyst having stored ammonia helps at converting the NOx not stored on the NSR catalyst. The Ford patent claims a NSR catalyst composed of noble metals deposited on a NOx-trap materials (alkali, alkali earth metals,…) while the SCR catalyst would be made of zeolite, silica–alumina, or titania promoted by Cu, Fe, or Ce. This system was further detailed in a patent in 2008 [47]. Chigapov et al. from Ford Germany recently published a patent in which special compositions of the LNT catalyst (based on rare-earth and earth alkaline oxides) and of the SCR catalyst (Cu–Ce zeolites) were claimed for a better use in LNT–SCR coupling [48]. The coupling between a NSR and a SCR catalyst was also claimed by Engelhardt [49]. A more general system in which the SCR catalyst could be coupled to NSR and oxidation catalysts and associated with a soot filter was patented by BASF [50]. In this patent, the claimed SCR catalyst is composed of silver tungstate Ag_2WO_4 supported on alumina. Other BASF patents were published in 2010 and 2011 to cover the specific case of NSR–SCR coupling systems [51, 52]. A NSR–SCR coupling system was also depicted by Johnsson–Matthey [53]. Indeed, recently Twigg et al. suggest the development of a multicomponent diesel catalyst known as "four-way catalysts" (FWCs) [54]. SCR and/or NOx-trapping components will be incorporated into catalysed filters from diesel cars in order to be cost-effective, weight effective, and space-effective. Finally, in the last 10 years, great efforts were made at Eaton Corporation to propose a viable technology with different configurations. No less than six patents were published by this Company claiming both depollution systems and catalysts for each configuration [55–60]. The systems may include two LNT bricks in parallel with optimization (i) of thermal changes during working and desulfation and (ii) of rhodium usage in the LNT catalyst.

Table 19.2 Effect of the addition of mordenites to Pt catalysts (2 % Pt/Al_2O_3 or 2 % Pt/CeO_2) for NOx conversion in cycled conditions (physical mixture of 80 part of MOR–20 and 20 part of Pt catalyst)

Catalyst	NOx conversion at various temperatures				
	200 °C	250 °C	300 °C	350 °C	400 °C
NSR alone	22.0	77.2	94.9	95.3	96.5
Pt/Al_2O_3 + MOR	19.6	28.4	27.1	14.5	5.4
Pt/CeO_2 + MOR	41.8	75.7	68.6	47.5	32.8
Conv. to N_2	28.6	38.5	49.0	41.8	18.4

Comparison with a NSR catalyst alone (2 wt.% Pt/75 % alumina-21 wt.% $BaCO_3$–2 wt.% K_2CO_3). From Ref. [61] selectivities are not detailed in this reference

19.3.2 Coupling of Pt Catalysts with Zeolites

Addition of nonpromoted zeolites to a NSR catalyst was investigated by Nakasutji et al. [61]. They showed that mordenites with a SiO_2/Al_2O_3 molar ratio of 10 or 20 were able to store significant amount of ammonia during the NOx-trap/reduction process and to improve NOx conversion. Preliminary experiments were carried out in a rich gas (400 ppm NO + 1 % H_2) and in simplified lean/rich cycles (lean: 2000 ppm NO + 8 % O_2; rich: 2 % H_2). They revealed that Pt/Al_2O_3 (without Ba) was able to produce ammonia during the rich phase (NO/H_2 mixture) and that MOR–10 or 20 could store ammonia in similar conditions. In spite of these reactive and adsorptive properties, the physical mixture composed of 20 parts Pt/Al_2O_3 and 80 parts of MOR–20 is much less efficient for NOx conversion than a standard NSR catalyst (Table 19.2). This is due to the very poor NOx-trap properties of the $Pt–Al_2O_3$: as there is no NOx trapped on the Pt catalyst, no ammonia could be produced during the rich phase. By contrast, the conversion is much higher when Pt/Al_2O_3 is replaced by Pt/CeO_2 which possesses significant NOx-trap capacity. Ammonia stored on the mordenite contributes for 50, 45, and 30 % of NOx conversion at 200, 300, and 400 °C, respectively. Unfortunately, relatively large amounts of N_2O are produced at 200–300 °C, which limits the conversion to N_2.

19.3.3 Coupling of Pt(RhPd)/BaO/Al_2O_3 with Cu–Zeolite Catalysts

The NSR–SCR coupling was studied by Shinjoh et al. who used Cu–ZMS5 as the SCR catalyst [62]. A three-bed reactor was developped comprising successively: a 2.4 % Pd/γ–Al_2O_3 catalyst (simulating the Diesel Oxidation Catalyst), the NSR catalyst (1.6 % Pt–0.16 % Rh/BaO/Al_2O_3) and the SCR catalyst (5 % Cu–ZMS–5). The catalyst performances were compared in lean/rich cycled conditions (3 min each). A significant beneficial effect of adding Cu–ZMS5 to the Pd + NSR

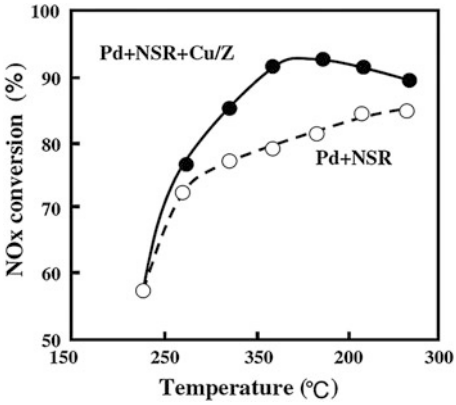

Fig. 19.4 Effect of Cu–ZSM-5 added to the Pd + NSR catalyst. *Lean gas* 230 ppm NO, 6.5 vol % O_2, 9.6 vol % CO_2, 3 vol % H_2O balanced N_2, *Rich gas* 230 ppm NO, 0.4 vol % O_2, 3,900 ppmC with C_3H_6 as HC, 9.6 vol % CO_2, 3 vol % H_2O balanced N_2

catalyst was observed between 230 and 310 °C. The increase of conversion can amount to +15 % when Cu–ZSM-5 is added (Fig. 19.4).

The role of each catalyst was detailed by Shinjoh et al. The **Pd catalyst** allows the NO oxidation into NO_2 in the lean phase (reaction 19.15) and significantly increases the NH_3 formation during the rich phase (reaction 19.16):

$$\text{Lean} \quad \text{NO} + \text{O}_2 \rightarrow \text{NOx} \tag{19.15}$$

$$\begin{aligned}\text{Rich} \quad \text{NOx} + \text{Red}(\text{H}_2, \text{CO}, \text{HC}) &\rightarrow \text{NH}_3 + \text{H}_2\text{O} + \text{CO}_2 \\ &\rightarrow \text{N}_2 + \text{H}_2\text{O} + \text{CO}_2\end{aligned} \tag{19.16}$$

A third role of the Pd catalyst is to catalyze partial oxidation of propylene in reducing conditions, C_3H_6 being then partially transformed into H_2 and CO. The **NSR catalyst** stores the NOx during the lean phase (reaction 19.17) and forms N_2 or NH_3 during the rich phase (reaction 19.18).

$$\text{Lean NOx} \rightarrow \text{NOx}_{(\text{ad})} \tag{19.17}$$

$$\begin{aligned}\text{Rich NOx}_{(\text{ad})} + \text{Red}(\text{H}_2, \text{CO}, \text{HC}) &\rightarrow \text{N}_2 + \text{H}_2\text{O} + \text{CO}_2 \\ &\rightarrow \text{NH}_3 + \text{H}_2\text{O} + \text{CO}_2\end{aligned} \tag{19.18}$$

Finally, the **SCR catalyst** stores ammonia during the rich phase (reaction 19.20) and allows the reaction of adsorbed ammonia with NO not converted in the lean phase (reaction 19.19).

$$\text{Lean NOx} + \text{NH}_{3(\text{ad})} \rightarrow \text{N}_2 + \text{H}_2\text{O} \tag{19.19}$$

$$\text{Rich}: \ \text{NH}_3 \rightarrow \text{NH}_{3(\text{ad})} \tag{19.20}$$

The effect of Cu–ZSM-5 (5 % Cu) addition on the performances of Pt–Rh/BaO/Al_2O_3 (Pt–RhBa) catalyst was also investigated by Corbos et al. [63, 64]. The catalytic system was tested in periodic cycling conditions (100 s lean/10 s rich) between 200 and 400 °C in three configurations: NSR catalyst alone, physical

Table 19.3 Effect of adding a SCR catalyst (Cu/ZSM-5) to a NSR catalyst (Pt–Rh/Ba) in cycling conditions: 100 s lean (500 ppm NO + 0.13 % CO/H_2 + 167 ppm C_3H_6 + 1 % CO_2 + 10 % O_2 in He) and 10 s rich (100 ppm NO + 8.53 % CO/H_2 + 1 % CO_2 in He)

Reductant	Catalyst	NOx removal		
		250 °C	300 °C	400 °C
CO/H_2 mixture	Pt–Rh/Ba (NSR alone)	39	50	39
	CuZSM-5	11	13	–
	Pt–Rh/Ba + CuZSM-5 (2 beds)	46	61	37
	Pt–Rh/Ba + CuZSM-5 (phys. mix.)	86	79	38
Pure CO (6.4 %)	Pt–Rh/Ba (NSR alone)	39	43	36
	Pt–Rh/Ba + CuZSM-5 (2 beds)	39	58	42
	Pt–Rh/Ba + CuZSM-5 (phys. mix.)	54	66	45
Pure H_2 (6.4 %)	Pt–Rh/Ba (NSR alone)	47	54	48
	Pt–Rh/Ba + CuZSM-5 (2 beds)	67	73	42
	Pt–Rh/Ba + CuZSM-5 (phys. mix.)	68	77	45
Pure H_2 (2.14 %)	Pt–Rh/Ba + CuZSM-5 (2 beds)	62	60	–
	Pt–Rh/Ba + CuZSM-5 (phys. mix.)	67	61	–

The gas mixture CO/H_2 contains 75 % CO and 25 % H_2

mixture of NSR + CuZSM-5 or dual bed catalyst (CuZSM-5 downstream NSR). The results are shown in Table 19.3.

While Cu–ZSM-5 is almost inactive in NOx abatement in NSR cycling conditions, addition of this catalyst to Pt–Rh/Ba improves the performance of the NSR catalyst at 250 and 300 °C. At 400 °C, there is virtually no improvement when Cu–ZSM-5 is added to the NSR catalyst. At this temperature, ammonia is either not produced or not stored on the SCR catalyst. Interestingly, the physical mixture of Pt–Rh/Ba and CuZSM-5 gives better performances than the dual bed system. Corbos et al. concluded that a close proximity of the NSR catalyst with the NH_3–SCR catalyst was required for a better production and use of ammonia produced during the rich phase. The greatest effect of Cu–ZSM-5 is observed in the presence of H_2 in the reductant mixture, independently of the catalyst configuration (physical mixture or two beds). This is in line with H_2 giving the highest yield of ammonia in NSR cycling conditions. However, a cooperative effect between H_2 and CO can be observed at low temperature on the physical mixture, the reductant efficiency being in the following order: CO/H_2 mixture > H_2 alone > CO alone. However, most experiments were carried out in the absence of water in the synthetic gas. Adding 1 % H_2O in the gas mixture did not cause great difference in NOx removal over the NSR catalyst alone while a slight decrease in activity of the NSR–SCR catalyst combination was observed. Another critical point is the process selectivity: residual NH_3 is a criterion of the NSR–SCR efficiency (ammonia slip cannot be accepted) while N_2O formation is a good criterion of the reduction selectivity (N_2O is a powerful greenhouse effect gas). Figure 19.5 shows the NH_3 and N_2O concentration after the NSR catalyst and in the NSR–SCR configuration.

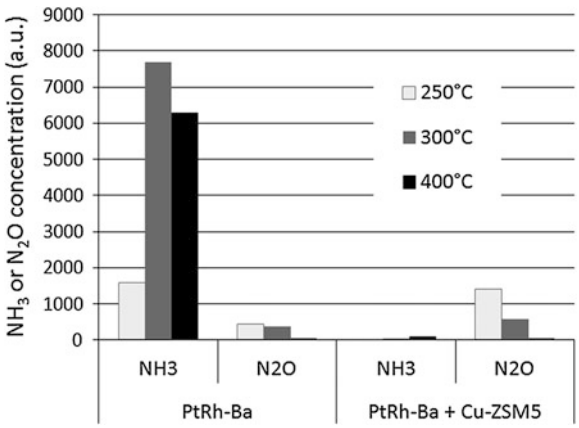

Fig. 19.5 Selectivity to NH_3 and N_2O of the NSR catalyst alone and in the NSR–SCR dual bed configuration. Gas compositions during lean and rich phases are detailed in Table 19.3

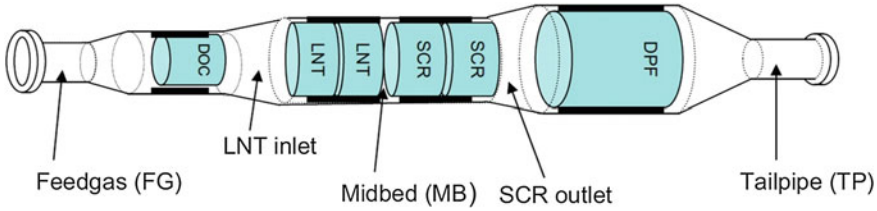

Fig. 19.6 System used in the vehicle tests [67]

A similar system (Pt–Rh NSR + Cu–zeolite) was recently investigated by Mc Cabe et al. [65–67] of Ford Motor Company. Figure 19.6 shows the implementation of the catalysts in the exhaust line for the engine tests.

Using a CO + H_2 + C_3H_6 mixture as the reductant in cycling experiments, NOx conversion was higher than with ammonia alone. Wang et al. concluded that propylene was an efficient reductant in the NSR–SCR combination. The results of a representative engine test over a high-emitting engine (called LR3) are given in Table 19.4. Though the SCR catalyst shows a non-negligible activity in converting NMHC (nonmethanic HC) and CO, the greatest effect can be observed on the NOx conversion. Only the LNT + SCR configuration allows to reach a good level of NOx abatement.

Separate experiments proved that Cu–zeolite was a good catalyst for NOx reduction, both by ammonia and alkenes. High resistance to deactivation by hydrocarbon and sulfur was obtained with a new generation of Cu–zeolite (Cu–CHA) which shows higher performances than the catalyst of the first generation composed of Fe–BEA [66, 67]. The NSR–SCR system is more efficient than the NSR catalyst alone up to 425 °C. Above this temperature, the SCR catalyst has no effect and it is advantageous to increase the loading of the NSR catalyst. However, such high temperatures are rarely encountered with normal diesel engine operation.

Table 19.4 Emission results from FTP test (Federal test procedure) over the LR3 engine (code location: see Fig. 19.6)

Emissions	Before DOC (FG) g/mile	After LNT (MB) g/mile	Tailpipe (TP) g/mile	DOC + LNT efficiency (%) (FG-MB)	SCR efficiency (%) (MB-TP)	Overall efficiency (%) (FG-TP)
NMHC	2.33	0.23	0.07	90	69	97
CO	6.42	0.30	0.21	95	30	97
NOx	1.02	0.25	0.07	78	74	93

Efficiency (%) represents the percentage of pollutant abatement (NMHC, CO, or NOx) at different stages of the exhaust pipe. From Ref. [67]

Table 19.5 NOx conversion, N_2, NH_3 and N_2O formation (expressed in N atoms) over the NSR catalyst alone and in the NSR + SCR configuration

T (°C)	NSR alone				NSR + Cu–ZSM-5 (left) and NSR + Cu–BEA (right)							
	NO conv (%)	N_2 form (%)	NH_3 form (%)	N_2O form (%)	NO conv (%)		N_2 form (%)		NH_3 form (%)		N_2O form (%)	
200	40.9	9.8	28.8	2.3	74.5	*63.5*	70.8	*48.7*	1.7	*12.8*	2.0	*2.0*
250	47.3	27.1	19.5	0.7	73.6	*77.3*	72.2	*73.0*	0.2	*1.8*	1.2	*2.5*
300	50.0	32.4	17.2	0.4	72.3	*71.4*	71.6	*70.3*	0.1	*0.3*	0.6	*0.8*
400	39.1	29.4	9.4	0.3	50.9	*52.5*	50.4	*51.7*	<0.1	*0.1*	0.5	*0.7*

Lean gas 750 ppm NO + 9.5 %O_2 (balance in Ar). *Rich gas* 750 ppm NO + 4 % H_2 (balance in Ar). Cycles: 150 s lean/20 s rich. Space velocity: 28,600 h^{-1} for NSR and 90,000 h^{-1} for SCR (1.4 % Cu/ZSM-5 or 2.1 % Cu/BEA). From Ref. [68]

The efficiency of Cu–BEA and Cu–ZSM-5 as SCR catalyst coupled with Pt/BaO/Al_2O_3 was compared by De La Torre et al. in a very recent paper [68]. Both zeolites lead to very active co-catalysts in promoting the NOx reduction by the NSR catalyst alone. The optimal Cu loading is obtained for 1.4 % Cu in ZSM-5 and 2.1 % Cu in BEA (Table 19.5). Cu–ZSM-5 and Cu–BEA can increase the NOx conversion by 20–30 % in the 200–300 °C temperature range. A significant formation of ammonia is observed on the NSR catalyst alone which is used for the SCR reaction (a part of NH_3 being oxidized by O_2). Cu–ZSM-5 and Cu–BEA have very similar effects so that activity per Cu ions appears higher over Cu–ZSM-5.

The two zeolite catalysts were characterized by De La Torre et al. [68]. Total acidity is higher over BEA but ZSM-5 shows a higher number of strong acid sites desorbing ammonia beyond 220 °C. In the optimized catalysts (1.4 % Cu–ZSM-5 and 2.1 % Cu–BEA), all the copper remains in the Cu^{2+} state. Increasing Cu loading leads to $H_2/Cu < 1$ in TPR experiments, which confirms the formation of Cu^+ and may be Cu^0 species. Reduced species of copper appear to be less active and less selective to N_2 (higher formation of N_2O).

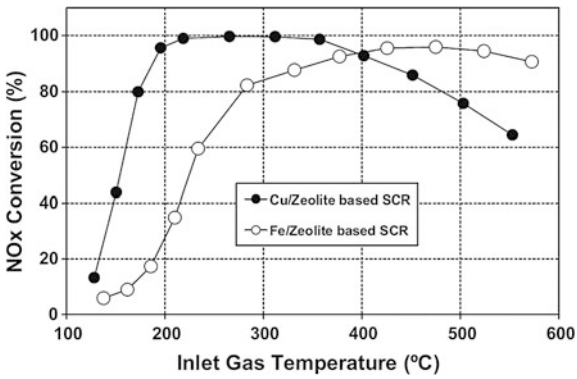

Fig. 19.7 NOx conversion in NH_3–SCR over zeolite catalysts after hydrothermal ageing for 64 h at 670 °C. Reaction conditions: 350 ppm NO, 350 ppm NH_3, 14 % O_2, space velocity: 30,000 h^{-1}. From Ref. [67]

19.3.4 Coupling of Pt(RhPd)/BaO/Al_2O_3 with Fe–Zeolite Catalysts

Systems coupling NSR with Fe–zeolite SCR catalysts were studied by many authors, in particular the Group of Forzatti in Milano [69–71], the Group of Daimler AG [72–75] and others [76–78]. Fe–zeolite are generally found less active in SCR than Cu–zeolite catalysts at low temperatures (Fig. 19.7) but they would be more selective to N_2. However, depending on the nature of the zeolite, contrasted results were obtained: for instance, Cu–ZSM-5 was shown to be slightly more selective than Fe–ZSM-5 when washcoated in dual layer monolith/NSR/SCR [79].

Kinetic studies and specific experiments with designed reactants coupled to FTIR or DRIFT were mainly employed by Forzatti and coworkers to get detailed information about the behavior of each catalyst configuration (Pt–Ba/Al_2O_3 alone, Fe–ZSM-5 alone or Pt–Ba/Al_2O_3 + Fe–ZSM-5). As expected, NOx is mainly stored on the basic NSR catalyst while ammonia formed upon the rich phase is mainly stored on the acidic SCR catalyst. Gaseous NOx slipped from the LNT catalyst during the lean phase reacts with NH_3 stored on Fe–ZSM-5 to give N_2. This classical view of the NSR–SCR system can lead to different performances depending on the proximity of the NSR and SCR catalysts (physical mixture vs. dual bed) and on the presence or not of CO_2 and H_2O in the gas mixture. Tables 19.6 and 19.7 summarize the result of Castoldi et al. [71]. Prolonged rich and lean phases (40 min each) were carried out with intermediary He purges to have a clearer analysis of the compounds stored and formed during each phase. Adding the SCR catalyst has a significant positive effect on the NOx removal, in the presence and in the absence of CO_2 and water in the gas mixture. This effect is slightly more marked when both catalysts are physically mixed, which is in line with the results of Corbos et al. [63]. However, though the dual bed system seems less effective for NOx removal, it leads to a higher selectivity to N_2 in rich phase, when there is no CO_2 and H_2O and in both phases (lean and rich) in the presence of CO_2 and H_2O.

Table 19.6 Quantitative analysis of lean/rich experiments performed over the NSR, NSR + SCR physical mixture and NSR/SCR dual bed configurations in the absence of CO_2 and H_2O

Amounts (μmol/gcat)	NSR alone	NSR + SCR (phys. mix)	NSR + SCR (dual bed)
NOx removed(a)	429	512	472
NOx stored(a)	429	434	423
N_2 (lean)	0	78	49
N_2 (rich)	193	51	209
NH_3 slip	57	70	14

Experimental conditions: T = 250 °C; lean phase NO (1,000 ppm) in O_2 (3 % v/v) + He; rich phase H_2 (2,000 ppm) in He; catalyst weight 60 mg LNT (or 60 mg NSR + 60 mg SCR); total flow rate 100 Ncm^3 /min mol/gcat refers to NSR Pt–Ba/Al_2O_3 weight. From Ref. [71]

The results of Tables 19.6 and 19.7 were obtained at 250 °C. In the physical mixture, the amount of removed NOx decreases with the temperature in the absence of CO_2 and H_2O while it is almost constant with CO_2 and H_2O. At 350 °C, there is virtually no difference when there is CO_2 + H_2O or not in the gases. In the dual bed, the amount of removed NOx tends to increase with temperature in every cases (with CO_2 + H_2O or not).

The effect of the reactor configuration (dual bed vs. physical mixture) seems to strongly depends on the temperature: in a preliminary study carried out at 200 °C, Bonzi et al. showed that NOx conversion was significantly higher in the physical mixture configuration, with 390, 610, and 980 μmol NOx removed/g respectively after the NSR catalyst alone, after the NSR–SCR dual bed and after the physical mixture [69]. A comparison with the results of Tables 19.6 and 19.7 shows that the differences between the three configurations are more marked at 200 °C than at 250 °C.

Following their patent publication (see Sect. 19.4.1), the Group of Daimler AG essentially worked at rationalizing the concept of smart catalytic converter by modeling the NSR–SCR dual bed [73, 74]. It was shown that a good adjustment of the NSR and SCR catalyst volume as well as a good balance between rich and lean cycle lengths are a prerequisite to an optimal operation of the system. An example of the modeling results, taken from Ref. [72], is given in Table 19.8. The model shows that increasing the SCR–to–NSR volume ratio (keeping constant the total volume) leads to a slight increase of the percent of NOx removal and to an increase of the amount of reacted ammonia (100 % in the second configuration of Table 19.8). The same model (COMSOL package) was used to optimize the lean/rich cycle duration.

Another modeling of the reactor volume was performed by Seo et al. [80] with a special insight to the formation of N_2O. In the NSR–SCR coupling, it is important to minimize (or annihilate) both ammonia and N_2O in the aftertreatment exhaust gas. This means that ammonia should be used to reduce NOx (or be oxidized to N_2) while N_2O, if formed, should be destroyed in the catalytic system. The NSR catalyst was composed of Pt/Pd/Rh/Ba/Ce/Zr on Al_2O_3 (relative

Table 19.7 Same results with 0.1 % CO_2 and 1 % H_2O in the gas mixture (*lean* and *rich*)

Amounts (μmol/gcat)	NSR alone	NSR + SCR (phys. mix)	NSR + SCR (dual bed)
NOx removed(a)	272	323	396
NOx stored(a)	272	307	272
N_2 (lean)	0	16	123
N_2 (rich)	93	21	135
NH_3 slip	117	7	0

Other conditions are given in Table 19.6. From Ref. [71]

Table 19.8 NOx removal efficiency and percentage of ammonia used to reduce NOx in a smart catalytic converter based on Pt–Ba–NSR and Fe–zeolite SCR catalyst

Catalyst configuration Respective volumes	% NOx removed on the NSR unit	% NOx removed on the SCR unit	NH_3 reacted/NH_3 adsorbed
2 V of NSR + 1 V of SCR	55	7	0.3
1 V of NSR + 2 V of SCR	48	15	1.0

Reaction conditions: 240 °C, 165 s lean (500 ppm NO + 8 % O_2 + 8 % CO_2 + 8 % H_2O), 7 s rich (500 ppm NO + 1.6 % O_2 + 1.4 % H_2 + 0.3 % C_3H_6 + 4.2 % CO + 11.5 % CO_2 + 8 % H_2O). From Ref. [72]

weight− %: 3.3/0.72/0.31/12.56/7.97/4.49) while the SCR catalyst was a Fe–TMI zeolite (1.8 % Fe). Although it is not the best configuration in terms of NOx abatement, the system with an equal volume of NSR and SCR catalysts shows the best result in terms of ammonia and N_2O slip. A similar configuration was adopted by Pereda–Ayo to study the NSR (Pt–Ba–Al_2O_3)–SCR (Fe–BEA zeolite) coupling [78]. Nine values of nine parameters (81 experiments) were chosen to construct the abacus for predicting optimal performances. Very critical points are the temperature, the duration of lean-rich cycles and the concentration of H_2 in the respective lean and rich phase. It was shown that there is an optimum value of H_2 concentration (3 % in the conditions of Ref. [78]) to get the highest NOx conversion and the complete use of the ammonia produced in the NSR catalyst (no NH_3 slip). The specific role of H_2 concentration was also investigated by Lindholm et al. [76] who showed that the optimum H_2 concentration depended on the process temperature. A higher hydrogen concentration enhances the NOx removal efficiency at lower temperatures while this concentration should be reduced at higher temperatures to avoid an excess of ammonia leading to inhibition of the SCR reaction. Lindholm also showed that the NO_2/NO ratio was a critical factor in the NSR–SCR coupling. There is a clear benefit when NO_2 is present in the feed at low temperatures. Model studies were recently performed by Kota et al. who investigated the effect of exhaust pipe architecture (several sequential bricks LNT/SCR), the effect of the lean/rich cycle duration and the possible role of nonuniform noble metal loading [81]. The juxtaposition of two sequences of LNT/SCR bricks has a positive effect on NOx conversion while nonuniform metal loading has only a minor effect.

On the other hand, the lean/rich cycle duration has an important effect on the catalyst performance: reducing the cycle duration by a factor 2 can improve the NOx conversion by about 15–20 %.

19.3.5 Other Systems Including Tungsten-Based Catalysts

Sullivan and Keane have proposed a system in which both NSR and SCR components are included in the same materials [82]. Ba–ZSM-5 (4.3 % Ba), Fe–ZSM-5 (0.8 % Fe) and Ba–Fe–ZSM-5 were studied to evaluate the benefit of the concept. Oxygen is required to desorb NOx previously adsorbed on the catalyst, while gaseous ammonia is able to react with this stored NOx. Interestingly, Sullivan and Keane showed that N_2O was produced in the NH_3(g)/NO(a) reaction on Ba–ZSM-5 and Fe–ZSM-5, but to a lesser extent on the composite FeBa–ZSM-5 catalyst.

Corbos et al. investigate the coupling of Pt–Rh/Ba/Al_2O_3 with different potential SCR catalysts (Co/Al_2O_3, CuZSM-5, Ag/Al_2O_3) [64]. As expected (and already found in a previous work [63]), addition of Cu–ZSM-5 gave the highest performances. Excellent performances were also obtained with Co/Al_2O_3 while addition of Ag/Al_2O_3 had no significant influence. The negative effect of water on the global performances of Pt–Rh/Ba/Al_2O_3 + Cu–ZSM-5 was ascribed to an inhibition of the reactions occurring on Cu–ZSM-5.

Berland et al. also studied the combination of a model NSR catalyst (1 % Pt/10 % BaO/Al_2O_3, denoted as Pt/Ba–Al) with oxides-based SCR samples [84]. WO_3 supported over ceria-zirconia oxides (WO_3/Ce–Zr) were studied as the active NH_3–SCR catalysts. The effect of the composition of the ceria-zirconia mixed oxides was studied with a constant WO_3 loading (10 wt.% of W, added by impregnation). It is demonstrated that Pt/Ba–Al NSR catalyst can release important amount of ammonia, until over 50 % of selectivity at 300 °C (Fig. 19.8a). SCR materials WO_3/Ce–Zr, with different Ce–Zr ratio, were associated downstream to the Pt/Ba–Al NSR catalyst. In the NSR + SCR combined system, the DeNOx efficiency is strongly improved. An enhancement of 24 points in NOx conversion was obtained at 300 °C for the better SCR sample (WO_3/Ce–$Zr_{(20–80)}$) (Fig. 19.8b) [83].

The acidic, basic, and redox properties of the SCR catalysts were investigated. In fact, it is reported in Ref. [85] that the redox properties are the key factors controlling the reactivity of the catalysts at low temperature, whereas at high temperature the acid properties are expected to play a major role in the SCR reaction. The addition of well-dispersed surface WO_3 to CeO_2–ZrO_2 oxide led to an important NH_3 storage capacity (acidity) not present on the host support. In the same time, the addition of tungsten trioxide strongly decreased the oxygen mobility, the NO to NO_2 oxidation activity and NOx storage capacity of ceria-zirconia oxides. The NOx selective catalytic reduction with ammonia (NH_3–SCR) and the NH_3 selective catalytic oxidation with oxygen (NH_3–SCO) behaviors of these SCR samples have been also studied [83]. All WO_3/Ce–Zr materials are active for reducing effectively the NOx. These solids can reduce more than 80 %

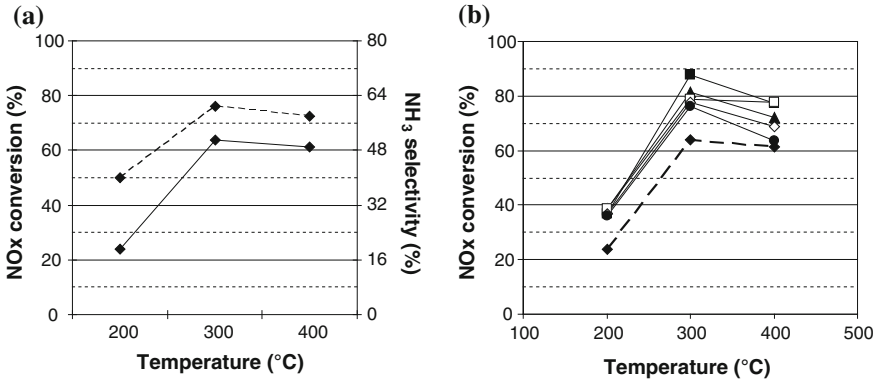

Fig. 19.8 **a** NOx conversion (—) and NH_3 selectivity (–) over NSR Pt/Ba–Al model catalyst. **b** NOx conversion in NSR + SCR (NSR:SCR = 60:120) combined system, from [83]: (◆): Pt/Ba–Al; (■): Pt/Ba–Al + WO_3/Ce–Zr(20–80); (▲): Pt/Ba–Al + WO_3/Ce–Zr(40–60); (□): Pt/Ba–Al + WO_3/Ce–Zr(58–42); (◇): Pt/Ba–Al + WO_3/Ce–Zr(70–30); (●): Pt/Ba–Al + WO_3/CeO[2]. *Lean* (60 s): 500 ppm NO + 10 % O_2 + 10 % CO_2 + 10 % H_2O, *Rich* (3 s): 3 % H_2 + 10 % CO_2 + 10 % H_2O

of NOx in NH_3–SCR conditions including CO_2 and H_2O in feed gas. A strong oxidation of ammonia was also reported in the absence of NOx with nearly 80 % of ammonia oxidized only into nitrogen.

Placed downstream to a model Pt/Ba–Al NSR catalyst, it was demonstrated that the NH_3 reactivity is temperature-dependent. At low temperature (200 °C), all the emitted ammonia from the NSR catalyst reacts (Fig. 19.8c), but according only to the standard NH_3–SCR (see Sect. 19.4.1). At higher temperature, fast NH_3–SCR is then favored due to the NO oxidation into NO_2 over the upstream NSR bed. Besides, at 300 and 400 °C, a part of the stored ammonia is converted into N_2 via the SCO reaction (Fig. 19.9b). In addition, some NH_3 is released, especially for lower Zr contents in WO_3/Ce–Zr materials (WO_3/Ce–$Zr_{(58-42)}$ and WO_3/Ce–$Zr_{(70-30)}$). This result implies competitions between the NH_3–SCR and the NH_3–SCO reactions together with the formulation of WO_3/Ce–Zr SCR samples (Fig. 19.9a and b). It also puts in evidence a lack of strong acid sites in order to store NH_3 at high temperature.

Finally, the work of Kim et al. about the HC–SCR and NH_3–SCR coupling system should be mentioned [86]. Although this study is out of the scope of the present chapter, it obeys to the same principle: the first bed (composed of Ag/Al_2O_3) is active in NOx reduction by hydrocarbons or alcohols but it produces also ammonia and HCN which can be used in the second bed (CuCoY or Pd/Al_2O_3) in order to reduce the unconverted NOx by ammonia.

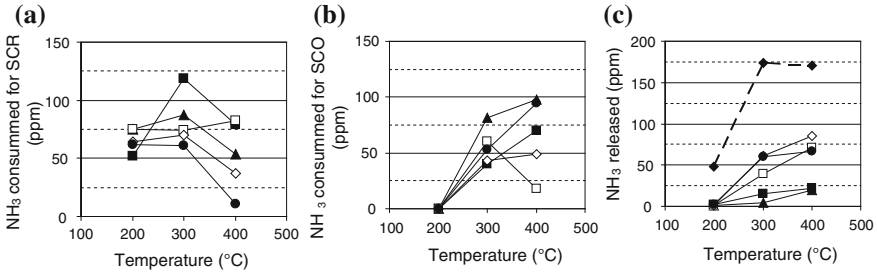

Fig. 19.9 Ammonia consumption (ppm) on WO_3/Ce–Zr SCR catalyst in NSR + SCR (NSR:SCR = 60:120) combined system for (**a**) NH_3–SCR (**b**) NH_3 SCO and (**c**) unconverted NH_3 [83]. (◆): Pt/Ba–Al; (■) Pt/Ba–Al + WO_3/Ce–Zr(20–80); (▲): Pt/Ba–Al + WO_3/Ce–Zr(40–60); (□): Pt/Ba–Al + WO_3/Ce–Zr(58–42); (◇): Pt/Ba–Al + WO_3/Ce–Zr(70–30); (●): Pt/Ba–Al + WO_3/CeO_2, *Lean* (60 s): 500 ppm NO + 10 % O_2 + 10 % CO_2 + 10 % H_2O, *Rich* (3 s): 3 % H_2 + 10 % CO_2 + 10 % H_2O

19.4 Selective Catalytic Reduction of NOx by Ammonia (NH_3–SCR)

As illustrated previously, materials associated downstream to the NSR catalysts are usually metal-exchanged zeolites [87], or more recently acidic ceria-zirconia based oxides as NH_3–SCR catalysts [83]. These samples have to be active in NOx reduction by NH_3 together with a high ammonia storage capacity. Thus, zeolite type structure was largely studied in the coupling NSR + SCR system. More specifically, iron and copper are the main exchanged metal in zeolites. Among the possible zeolites, ZSM-5 is one of the most studied materials in the academic literature, even if it is not the more appropriate structure.

19.4.1 Mechanistic Aspects of the SCR Reaction

The reaction pathway of the NOx selective catalytic reduction with ammonia (NH_3–SCR) is described by the following reactions (reactions 19.21–19.24):

$$4NH_3 + 4NO + O_2 \rightarrow 4N_2 + 6H_2O \quad (19.21)$$

$$4NH_3 + 2NO + 2NO_2 \rightarrow 4N_2 + 6H_2O \quad (19.22)$$

$$4NH_3 + 3NO_2 \rightarrow 3.5N_2 + 6H_2O \quad (19.23)$$

$$4NH_3 + 6NO \rightarrow 5N_2 + 6H_2O \quad (19.24)$$

These reactions are usually denoted as “standard” (19.21), “fast” (19.22), “NO_2–SCR” (19.23) and finally “slow” (19.24) SCR reactions [31, 88–91]. It is

usually established in the literature that SCR of NOx with NH_3 occurs through an Eley–Rideal type mechanism [92–97], in which adsorbed ammonia reacts with weakly adsorbed NO or NO in the gas phase. Nevertheless, some studies suggest a reaction following a Langmuir–Hinshelwood mechanism [98–100]. However, it is currently received that SCR chemistry over metal-exchanged zeolite firstly requires the NO oxidation into NO_2, which is claimed to be the rate-determining step of the SCR mechanism [101]. For this reaction, metal-exchanged zeolites present largely higher activity than transition metal free zeolites [102]. It is also clearly evidenced that the NO_2/NO ratio is a key parameter for the SCR activity [88, 89, 103–105]. Indeed, fast SCR (reaction 19.22) and NO_2–SCR (reaction 19.23) reactions are much faster than the standard NO–SCR reaction (reaction 19.21). Note that in a NSR + SCR coupling system, the high oxidation activity of the Pt(RhPd)/BaO/Al_2O_3 NSR formulation also provides NO_2 by the oxidation of NO. Transition metal centers on zeolite are not only involved in the NO oxidation. For instance, it is suggested that iron species also promote the SCR reaction over zeolite framework in the case of the Fe-exchanged ZSM-5 materials [106]. Especially, transition metal sites are claimed to promote the formation of reactive nitrates on the catalyst surface in the presence of gaseous NO_2 [107]. In fact, the formation of intermediate Fe^{n+}–NO species ($n = 2, 3$), $Fe^{2+}(NO)_2$ complexes, and NO^+ are reported [108]. Nitrosyl ion (NO^+) may be produced by N_2O_4 disproportionation, which is firstly formed by NO_2 dimerization. NO^+ can further react with H_2O to produce HNO_2. HNO_2 can then react with ammonia to produce ammonium nitrite (NH_4NO_2), which decomposes quickly below 100 °C, leading to the SCR products, N_2 and H_2O [109]. Ammonium nitrate can also be formed according to reactions 19.25–19.26:

$$2NO_2 + 2NH_3 \rightarrow NH_4NO_3 + N_2 + H_2O \tag{19.25}$$

$$NO_3^- + NH_4^+ \rightarrow NH_4NO_3 \tag{19.26}$$

In this later process, NH_3 is activated on zeolitic Brønsted acid sites, giving NH_4^+ ions [110]. This point is discussed below (Sect. 19.4.2). Ammonium nitrate thereafter decomposes into NO_2 and NH_3, as reported in reaction 19.27:

$$2NH_4NO_3 + NO \rightarrow 3NO_2 + 2\,NH_3 + H_2O \tag{19.27}$$

The combination of reactions (19.25) and (19.27) leads to the "fast" SCR, as reported above (reaction 19.22) [111].

However, if transition metal exchanged zeolites are active materials in NH_3–SCR, N_2O emission can be also observed. N_2O emission constitutes one of the main drawbacks of this system. For instance, Wilken et al. [112] reports a maximum N_2O production at 200 °C over Cu–Beta zeolite. Mechanism of N_2O emission is proposed to proceed through the decomposition of ammonium nitrates (reaction 19.28):

$$NH_4NO_3 \rightarrow N_2O + 2H_2O \tag{19.28}$$

Fast SCR conditions, and more especially high NO_2 concentrations, are also proposed to favor the N_2O formation at low temperature (i.e., $T \leq 350$ °C) [113] (reaction 19.29). Mechanism involving NO (reaction 19.30) is proposed to occur at higher temperature (i.e., $T \geq 350$ °C) [114].

$$6NH_3 + 8NO_2 \rightarrow 7N_2O + 9H_2O \tag{19.29}$$

$$4NH_3 + 4NO + 3O_2 \rightarrow 4N_2O + 6H_2O \tag{19.30}$$

Finally, over Fe/MFI, and generally on zeolite, it is reported in the literature that N_2 formation requires one nitrogen atom from a molecule of NOx, and a second nitrogen atom from ammonia molecule [115]. This observation is consistent with SCR reactions described in reactions 19.21–19.23.

19.4.2 Effect of Zeolite Framework

In the NH_3–SCR mechanism, ammonia is firstly adsorbed and activated as NH_4^+ ions on the Brønsted acid sites of the zeolite framework. Acidic properties are then a crucial factor that determines the SCR activity. Since zeolite acidity is affected by the Si/Al ratio, high Al contents in the framework are favorable to achieve high NOx conversions. Indeed, the Brønsted acid sites of the zeolite structure originate from aluminum centers [113, 116]. Besides, it appears that zeolite with small average pore diameter, as encountered in MFI, MOR, BEA, or FER materials, are the more active for NH_3–SCR reaction. In opposition, molecular sieves having larger pore size, including Y, USY, or MCM–41 structures, exhibit lower activities. It is proposed in the literature that the formation of an active complex $[NH_4^+{}_x][NO]$ (with $x = 1, 2$) during SCR is facilitated in small pores, without effect of reactant surface mobility [117, 118]. A second hypothesis to explain the differences observed with the pore size is the formation of higher concentrations of $3H–NH_4^+$ compound (NH_4^+ bonded to three hydrogen atoms) in small pore size support [119]. $3H–NH_4^+$ compound is also reported as an intermediate for the formation of the active $[NH_4^+{}_x][NO]$ complex during the NH_3–SCR reaction. In addition, the zeolite channels size can also influence the H–bonding with framework oxygen atoms [118]. For instance, FeY and FeMCM–41, with large pore sizes, show lower activities for NH_3–SCR than FeZSM-5.

Nevertheless, it is also proposed that the active sites for the NO SCR by ammonia over HZSM-5 are highly acidic extra–framework alumina. In opposition, for NO_2 reduction reaction, both framework and extra-framework alumina sites are suggested to be active sites [120].

On the basis of these results, it appears that the activity of zeolite materials is associated with two main properties [121]:

1. A shape selectivity effect, due to the molecular sieving properties associated with the well defined crystal pore size, in which a part of the catalytic active sites are located;
2. A strong Brønsted acidity of bridging Si–(OH)–Al sites, generated by the presence of aluminum inside the silicate framework.

19.4.3 Role of Acidic Sites

The role of the acidic sites was studied by Brandenberger et al. [122] using different Fe–ZSM-5 samples at equal exchange degree but different Brønsted acidities. This study reveals that the acidity of the catalyst is not a crucial factor to achieve high activity for NO SCR with NH_3. Brønsted acidity may not be required for the adsorption or activation of the ammonia molecule, but it is necessary to bind and disperse the transition metal ions. The form in which ammonia is adsorbed on the support is consequently not crucial. These observations are confirmed by Schwidder et al. [123]. Indeed, high reaction rates for the NH_3–SCR can be achieved with nonacidic catalysts. A promoting effect of acidity is noted for the catalysts that contain the iron in the most favorable structure (i.e., oligomeric Fe oxo clusters).

In fact, FTIR characterization of the ZSM-5 acidic properties shows that two types of hydroxyl groups are mainly detected, giving bands at 3,720 and 3,605 cm^{-1} [124]. Thermal activation temperature strongly affects acidic properties. By increasing the temperature, dehydroxylation of the zeolite is observed above 400 °C. It induces a decrease of the number of Brønsted acid sites, while an increase in strong Lewis acid sites is observed. The dehydration at high temperature irreversibly removes the more acidic hydroxyl groups. Dealumination of zeolitic framework is also reported to modify acidity. Ammonia adsorption and temperature programmed desorption over ZSM-5 (Si/Al = 11.8) are studied in Ref. [125]. Three different states of chemisorbed ammonia are distinguished, which show desorption peaks at around 80, 180, and 430 °C. The distribution of chemisorbed ammonia is also reported to depend on the catalyst pre-treatment or deactivation. Recently, it was proposed that adsorption of ammonia on Brønsted acid sites goes through co-adsorption of up to four ammonia molecules on one active site at low temperatures. In addition, only a fraction of the aluminum framework is evidenced to be able to bind ammonia as ammonium ion [126]. Consequently, the support can act mainly as a reservoir for ammonia molecules, which then migrate to the active sites in order to undergo the reaction with NOx.

In a comparative study of the NH_3–SCR reactions over a Cu–zeolite and a Fe–zeolite catalyst, Colombo et al. [127] observed that iron zeolite catalyst stores a lower amount of strongly bonded ammonia than copper zeolite (Fig. 19.10). In addition, authors claim a greater activity in the ammonia oxidation reaction for the copper zeolite, together with a less sensitivity to the NO_2/NOx ratio for the DeNOx

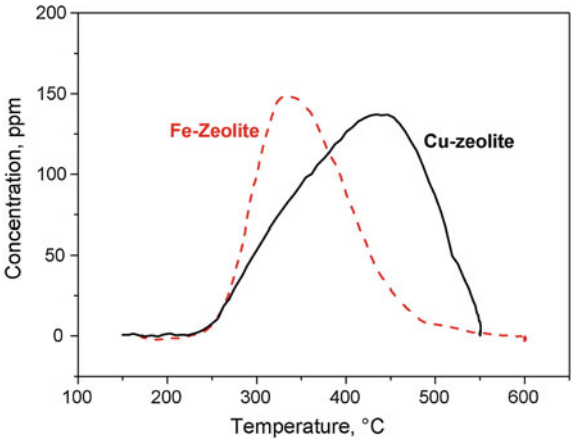

Fig. 19.10 Ammonia TPD over Cu- and Fe–zeolite: $Q = 71$ cm^3/min (STP), $H_2O = 3$ %, $O_2 = 0$ %, T ramp = 15 K/min. (*Solid line*) Cu–zeolite. (*Dashed line*) Fe–zeolite [127]

activity. Besides, N_2O is detected over Cu–zeolite even with negligible NO_2 feed content, whereas over iron zeolite, N_2O formation occurs only in excess of NO_2.

19.4.4 Active Sites and Performances of Cu–Zeolite, Fe–Zeolite, and Other Systems in NH_3–SCR

Although the identity and nuclearity of active sites is still in debate, Cu–zeolite binuclear species are clearly reported as active sites. Nevertheless, it seems that the nature of the copper active site is strongly influenced by the reaction temperature and by the properties of the used zeolite. Indeed, over FAU zeolite, $[CuOCu]^{2+}$ dimer species are proposed to catalyze NH_3–SCR reaction at low temperature ($T \leq 300$ °C) [128]. For NO decomposition, Moretti et al. [129, 130] also proposed that the main active sites over ZSM-5 (silica to alumina ratio from 66 to 80) consist of dimeric Cu species strongly anchored to "next-nearest-neighbor" framework AlO_4^- species. On the opposite, Cu^{2+} is suggested to become active at higher temperature ($T \geq 350$ °C) over NaY [131, 132].

At temperatures below 250 °C, Sjövall et al. [133] observed a beneficial effect of oxygen on the activity, contrary to higher temperatures. Ammonia slip is also affected by temperature. For instance, equal amounts of nitrogen oxides and ammonia are required at 175 °C. In fact, over Cu–ZSM-5 the NOx conversion is achieved by the reaction between NO_2 and adsorbed NH_3. At higher temperature, ammonia oxidation occurs. However, if exposing the catalyst to equimolecular amounts of NO and NO_2 increases the NOx conversion, N_2O formation is furthermore observed.

Unfortunately, Cu–ZSM-5 catalyst suffers from thermal and water deactivation leading to segregation of extra-framework copper ions, and/or to the sintering of CuO-like species. To improve the durability or the low-temperature activity,

Seo et al. studied the effect of ZrO_2 addition on DeNOx performance of a SCR Cu–ZSM-5 catalyst [134]. It is reported that incorporation of the appropriate amount of ZrO_2 (2 wt.%) increases the acid strength of acidic sites of catalyst which improved by 10–20 % the NOx conversion in the 200–300 °C temperature range, as well as the durability of Cu–ZSM-5 catalyst. Recently Kwak [135] reports that Cu^{2+} ion-exchanged SSZ–13 (Cu–SSZ–13 with Chabazite (CHA) structure, containing small radius (3.8 Å) eight-membered ring pores), is more active and selective in reducing NO with NH_3 compared to Cu–ZSM-5 and Cu–beta. For instance, after hydrothermal treatment at 800 °C for 16 h, Cu–SSZ–13 was found to show nearly no change in NOx reduction activity, while Cu–ZSM-5 and Cu–Beta were found to lose NOx reduction activity. In the same time, no significant rearrangement of nuclearity of copper active sites, of structural zeolite framework is observed on Cu–SSZ-13 compare to Cu–ZSM-5 after hydrothermal ageing.

In Fe/ZSM-5 (Fe/Al = 1), EXAFS characterization reveals the presence of diferric (hydr)oxo-bridged binuclear clusters, located at the ion-exchange positions of the zeolite, and compensating one or two lattice charges [136, 137]. For Fe/Al = 0.8, iron is predominantly present as large hematite particles, although a minor fraction of binuclear species might be present as well [136]. Small Fe_xO_y clusters like Fe_4O_4, isolated Fe^{2+} and Fe^{3+} ions, are also reported as possible active sites in the literature [138–141]. Besides, electron-deficient ferric oxide nanoclusters, isolated iron ions, and possibly oxygen-bridged iron binuclear complexes, may likewise coexist in Fe/MFI catalysts [142]. Finally, a high exchange level (M/Al ratio $\approx$ 1), which can be achieved with the CVD method for instance, confers activity at low temperature for the material. Additionally, a high metal content may lead to extra-framework metal oxide clusters, which can exhibit high activity for NH_3 oxidation [141]. In fact, the activity of Fe–ZSM-5 for SCR of NO by NH_3 is suggested to be catalyzed by different iron active species depending on temperature [143]. At temperatures below 300 °C, the SCR activity was observed to be primarily caused by monomeric iron sites. At higher temperature (T = 300–500 °C), the contribution of dimeric iron species, oligomeric species and partially uncoordinated iron sites become important. Fe–zeolite catalyst can also be sensitive to the NO/NO_2 ratio for NOx removal via ammonia SCR [144]. The SCR efficiency was greatly enhanced when using pure NO_2.

Other catalytic systems are also studied for the abatement of NOx by reaction with ammonia, namely vanadium oxide—titania based samples or transition metal oxide—based materials. On these catalysts, ammonia is activated by coordination over Lewis acid sites, and can react with NO from the gas phase or weakly adsorbed NO [102]. Over V_2O_5–$WO_3(MoO_3)/TiO_2$ materials, new relevant contributions appeared in the literature, in particular concerning the reaction mechanism and the role of preoxidation of NO to NO_2. Coordinated ammonia would be oxidized to amide species, which later reacts with NO to form adsorbed nitrosamide species. Nitrosamide species decomposes into nitrogen and water, while oxygen reoxidizes the catalyst surface [96]. Unfortunately, these catalytic systems remain poorly active at low temperature, and temperature higher than 350 °C is needed to achieve high NOx abatement. In order to increase the low

temperature activity, new formulations based on transition metal oxides are proposed. For instance, Mn and Fe oxides supported on titania and alumina are active in NH_3–SCR at low temperature (150–250 °C) [145]. However, the main drawback of these catalysts is the limited selectivity of the NOx conversion into N_2, with significant production of N_2O. In addition, vanadia-based catalysts are not suitable for high temperature application as it can be the case in automotive exhaust pipe. Indeed, the sublimation of V_2O_5 occurs from 650 °C [113, 118]. Then, new catalytic systems having high efficiency at low temperature, thermally stable up to 800 °C, and with a limited impact of the NO_2/NOx ratio on the activity, are developed. Amongst these new emerging SCR catalytic systems, acidic zirconia mixed-oxides are described as attractive alternatives [146]. For instance, 50 % NO conversion was attained at 250 °C for the standard SCR process. By applying the "fast" SCR conditions (NO_2/NOx = 50 %), 97 % of NOx were reduced to N_2 at only 200 °C [147]. The promotion of acidic zirconia by ceria also increases the NOx conversion, the selectivity to N_2 and the catalyst durability. These results show that modified acidic zirconia oxides are attractive materials for Diesel after treatment systems [146]. However, Fe or Cu exchanged zeolites, which exhibit high reactivity toward the NOx SCR by NH_3, are the more quoted materials for a coupling with a NSR catalyst.

19.5 Conclusion and Perspective

The combination of NOx trapping materials with NH_3–SCR catalysts for the NOx treatment from mobile lean-burn engines has been reported. Particular attention has been paid in the mechanism of ammonia emission and reactivity toward NOx abatement in NSR process. For the first point, two reaction paths are proposed in the literature. In the presence of hydrogen during the rich pulses of the LNT regeneration, ammonia can be formed by direct reaction with the previously stored NOx. When CO is use as the reductant agent, water-assisted reaction, by hydrolysis of intermediate isocyanate species, is suggested. In the presence of water and carbon dioxide in the gas mixture, both reaction pathways co-exist due to direct and reverse water gas shift reaction. Ammonia is thereafter involved in the NOx reduction mechanism, by a sequential route in which NH_3 reacts faster with NOx to yield N_2 compared with its own formation rate. It is found that both the nature and the content of the basic element as well as the redox properties of the support interfere in NH_3 yield.

Ammonia may likewise be used as reductant for selective catalytic reduction of NOx species. For this application, metal-exchanged zeolite catalysts offer new opportunities to reduce NOx emissions from lean-burn engine via the NH_3–SCR process. Iron-exchanged ZSM-5 has received much attention because of its promising activity and stability in the NH_3–SCR process. Correlating catalytic activities with the concentration of mononuclear and binuclear Fe species shows that both types of Fe ions and even small metal clusters are active sites for SCR,

but that isolated species are more active. The topology of the zeolite is also an important factor, as well as its stability under hydrothermal conditions. A high exchange level (M/Al ratio $\approx$ 1) seems to be proscribed creating extra-framework metal oxide clusters, which can be highly active for NH_3 oxidation.

The coupling between a NOx-trap catalyst and a NH_3–SCR material located downstream the first one or in a double layer on the monolith, was firstly patented by Ford in 2004. In other recent studies, two main SCR catalysts are usually associated in such system, namely Cu–ZSM-5 and Fe–ZSM-5 catalysts. For instance, it is reported that using Cu–ZSM-5 material, about 15–50 % of supplementary NOx conversion can be achieved, depending on the working conditions. Whatever the zeolite used, higher performances are reported with H_2 as reductants, since it enhances NH_3 formation in the first NSR catalytic bed. Physical mixture of NSR and SCR catalysts gives better performances than dual bed system. It is concluded that a close proximity of both materials was required for a better use of ammonia produced during the rich pulses.

Furthermore, in almost every case of lean-burn engine after-treatment implementation in the USA and Europe, a Diesel particulate filter (DPF) is required. The NSR + SCR system must be compatible with the DPF working mode. Filter regeneration induces severe exotherms (900–1000 °C) which expose NSR + SCR catalysts to harsh environment. To maintain the durability of this coupled system, the catalysts must exhibit high thermal stability. As a consequence, usual vanadia-based oxides SCR catalysts are not suitable. The stability of metal-exchanged zeolite has to be improved to prevent potential metal migration, or sulfur poisoning. A way is metal-exchanged in small-pore zeolites which shown to be much more hydrothermally stable than the medium-pore zeolite. New acidic zirconia-based oxides seem also attractive for this application.

Finally, the literature essentially focuses on the association of NSR catalyst with usual NH_3–SCR samples. However, in this coupled NSR + SCR system, ammonia is not directly injected in the feed gas, but produced during the regeneration step of the NSR process. The additional NOx reduction occurs during the lean phases (in O_2 excess) between NOx from gas phase and stored ammonia. It makes a prominent difference with the usual NH_3–SCR technology. The development of specific SCR catalyst is desirable in a near future to achieved DeNOx efficiency and nitrogen yield even higher.

References

1. Takeshima S, Tanaka T, Iguchi S, Araki Y, Hirota S, Oda T, Murakami F (1995) *Exhaust purification device of internal combustion engine.* US Patent 5,437,153 (Aug. 1, 1995)
2. Goto M, Iguchi S, Katoh K, Kihara T (1995) *Exhaust gas purification device for an engine.* US Patent 5,472,673 (Dec.5, 1995)
3. Takahashi N, Shinjoh H, Iijima T, Suzuki T, Yamazaki K, Yokota K, Suzuki H, Miyoshi N, Matsumoto S, Tanizawa T, Tanaka T, Tateishi S, Kasahara K (1996) *The new concept 3-way*

catalyst for automotive lean-burn engine: NOx storage and reduction catalyst. Catal. Today 27:63–69
4. Kobayashi T, Yamada T, Kayano K (1997) Study of NOx Trap Reaction by Thermodynamic Calculation. SAE Technical Papers 970745:63
5. Matsumoto S, (2000) *Catalytic reduction of nitrogen oxides in automotive exhaust containing excess oxygen by NOx storage-reduction catalyst*. Cattech 4:102–109
6. Roy S, Baiker A (2009) *NOx Storage-Reduction Catalysis: From Mechanism and Materials Properties to Storage-Reduction Performance*. Chem. Rev.*109:*4054–4091
7. Kwak JH, Kim DH, Szanyi J, Peden CHF (2008) *Excellent sulfur resistance of Pt/BaO/CeO2 lean NOx trap catalysts.* Applied Catal. B 84:545–551
8. Corbos EC, Elbouazzaoui S., Courtois X, Bion N, Marecot P, Duprez D (2007) *NOx storage capacity, SO2 resistance and regeneration of Pt/(Ba)/CeZr model catalysts for NOx-trap system*. Topics in Catalysis 42–43:9–13
9. Toops TJ, Smith DB, Epling WS, Parks JE, Partridge WP (2005) *Quantified NOx adsorption on Pt/K/gamma-Al_2O_3 and the effects of CO_2 and H_2O.* Applied Catal. B 58:255–264
10. Lesage T, Saussey J, Malo S, Hervieu M, Hedouin C, Blanchard G, Daturi M (2007) *Operando FTIR study of NOx storage over a Pt/K/Mn/Al_2O_3-CeO_2 catalyst*. Applied Catal. B 72:166–177
11. Szailer T, Kwak JH, Kim DH, Hanson JC, Peden CHF, Szanyi J (2006) *Reduction of stored NOx on Pt/Al_2O_3 and Pt/BaO/Al_2O_3 catalysts with H_2 and CO*. J. Catal. 239:51–64
12. Nova I, Lietti L, Forzatti P, Prinetto F, Ghiotti G (2010) *Experimental investigation of the reduction of NOx species by CO and H_2 over Pt–Ba/Al_2O_3 lean NOx trap systems*. Catal. Today 151:330–337
13. Kočí P, Plát F, Štěpánek J, Bártová Š, Marek M, Kubíček M, Schmeißer V, Chatterjee D, Weibel M (2009) *Global kinetic model for the regeneration of NOx storage catalyst with CO, H_2 and C_3H6 in the presence of CO_2 and H_2O*. Catal. Today 147:257–264
14. Masdrag L, Courtois X, Can F, Rohart E, Blanchard G, Marecot P, Duprez D (2012) *Understanding the role C3H6, CO and H2 on efficiency and selectivity of NOx Storage* 41 *Reduction (NSR) process: Activity during the lean period*. Catal. Today 189:70–76
15. Masdrag L, Courtois X, Can F, Duprez D. *Effect of reducing agents (C3H6, CO, H2) on the NOx conversion and N2O–NH3 selectivities during representative lean/rich cycles over platinum-based model NSR catalyst.* Submitted
16. Flura A, Can F, Courtois X, Royer S, Duprez D (2012) *Silver supported over high-surface-area zinc aluminate spinel as an active material in low-temperature SCR of NO with ethanol.*Applied Catal. B 126:275–289
17. Castoldi L, Lietti L, Forzatti P, Morandi S, Ghiotti G, Vindigni F (2010) *The NOx storage-reduction on PtK/Al2O3 Lean NOx Trap catalyst.* J. Catal. 276:335–350
18. Castoldi L, Nova I, Lietti L, Forzatti P (2004) *Study of the effect of Ba loading for catalytic activity of Pt–Ba/Al2O3 model catalysts.* Catal. Today 96:43–52
19. Artioli N, Matarrese R, Castoldi L, Lietti L, Forzatti P (2011) *Effect of soot on the storage-reduction performances of PtBa/Al2O3 LNT catalyst.* Catal. Today 169:36–44
20. Pereda-Ayo B, González-Velasco JR, Burch R, Hardacre C, Chansai S (2012) *Regeneration mechanism of a Lean NOx Trap (LNT) catalyst in the presence of NO investigated using isotope labelling techniques.* J. Catal., 285:177–186
21. Frank B, Emig G, Renken A (1998) *Kinetics and mechanism of the reduction of nitric oxides by H2 under lean-burn conditions on a Pt–Mo–Co/α-Al2O3 catalyst.* Appl. Catal. B. 19:45–57
22. Clayton RD, Harold MP, Balakotaiah V (2008) *NOx storage and reduction with H2 on Pt/BaO/Al2O3 monolith: Spatio-temporal resolution of product distribution.* Appl. Catal. B. 84:616–630
23. Breen JP, Burch R, Fontaine-Gautrelet C, Hardacre C, Rioche C (2008) *Insight into the key aspects of the regeneration process in the NOx storage reduction (NSR) reaction probed using fast transient kinetics coupled with isotopically labelled 15NO over Pt and Rh-containing Ba/Al2O3 catalysts.* Appl. Catal. B. 81:150–159

24. Bhatia D, Harold MP, Balakotaiah V (2010) *Modeling the effect of Pt dispersion and temperature during anaerobic regeneration of a lean NOx trap catalyst,* Catal. Today 151:314–329
25. Corbos EC, Courtois X, Can F, Marécot P, Duprez D (2008) *NOx storage properties of Pt/Ba/Al model catalysts prepared by different methods: Beneficial effects of a N2 pre-treatment before hydrothermal aging.* Appl. Catal. B. 84:514–523
26. Clayton RD, Harold MP, Balakotaiah V (2008) *Selective catalytic reduction of NO by H2 in O2 on Pt/BaO/Al2O3 monolith NOx storage catalysts.* Appl. Catal. B 81:161–181
27. Pereda-Ayo B, Duraiswami D, González-Marcos JA, González-Velasco JR (2011) *Performance of NOx storage–reduction catalyst in the temperature–reductant concentration domain by response surface methodology.* Chem. Eng. J. 169:58–67
28. Le Phuc N, Courtois X, Can F, Royer S, Marecot P, Duprez D (2011) *NOx removal efficiency and ammonia selectivity during the NOx storage-reduction process over Pt/BaO(Fe, Mn, Ce)/Al2O3 model catalysts. Part I: Influence of Fe and Mn addition.* Appl. Catal. B 102:353–361
29. Le Phuc N, Courtois X, Can F, Royer S, Marecot P, Duprez D (2011) *NOx removal efficiency and ammonia selectivity during the NOx storage-reduction process over Pt/BaO(Fe, Mn, Ce)/Al2O3 model catalysts. Part II: Influence of Ce and Mn–Ce additio*n. Appl. Catal. B 102:362–371
30. Choi JS, Partridge WP, Pihl JA, Daw CS (2008) *Sulfur and temperature effects on the spatial distribution of reactions inside a lean NOx trap and resulting changes in global performance.* Catal. Today 136:173–182
31. Nova I, Lietti L, Forzatti P (2008) *Mechanistic aspects of the reduction of stored NOx over Pt–Ba/Al2O3 lean NOx trap systems.* Catal. Today 136:128–135
32. Lietti L, Nova I, Forzatti P (2008) *Role of ammonia in the reduction by hydrogen of NOx stored over Pt–Ba/Al2O3 lean NOx trap catalysts.* J. Catal. 257:270–282
33. Lindholm A, Currier NW, Fridell E, Yezerets A, Olsson L (2007) *NOx storage and reduction over Pt based catalysts with hydrogen as the reducing agent: Influence of H2O and CO2.* Appl. Catal. B. 75:78–87
34. Le Phuc N, Courtois X, Can F, Berland S, Royer S, Marecot P, Duprez D (2011) *A study of the ammonia selectivity on Pt/BaO/Al2O3 model catalyst during the NOx storage and reduction process.* Catal. Today 176:424–428
35. Joubert E, Courtois X, Marecot P, Canaff C, Duprez D (2006) *The chemistry of DeNOx reactions over Pt/Al2O3: The oxime route to N2 or N2O.* J. Catal. 243: 252–262
36. Chen HY, Voskoboinikov T, Sachtler WMH (1999) *Reaction Intermediates in the Selective Catalytic Reduction of NOx over Fe/ZSM-5.* J. Catal. 186:91–99
37. Larson RS, Pihl JA, Chakravarthy VK, Toops TJ, Daw CS (2008) *Microkinetic modeling of lean NOx trap chemistry under reducing conditions*. Catal. Today 136:104–120
38. Le Phuc N, Corbos EC, Courtois X, Can F, Marecot P,.Duprez D (2009) *NOx storage and reduction properties of Pt/CexZr1−xO2 mixed oxides: Sulfur resistance and regeneration, and ammonia formation.* Appl. Catal. B. 93:12–21
39. Kinugasa Y, Igarashi K, Itou T, Suzuki N, Yaegashi T, Tanaka T (1998) *Device for purifying an exhaust gas of an engine*. US Patent 5782087 (Jul. 21, 1998)
40. Kinugasa Y, Itou T, Hoshi K, Suzuki N, Yaegashi T, Igarashi K (1999) *Device for purifying exhaust gas from engine*. US Patent 5964088 (Oct. 12, 1999)
41. Kinugasa Y, Igarashi K, Itou T, Suzuki N, Yaegashi T, Takeuchi K (2000) *Metho adsprobedd and device for purifying exhaust gas from engine*. US Patent 6047542 (April 11, 2000)
42. Kinugasa Y, Igarashi K, Itou T, Suzuki N, Yaegashi T, Tanaka T, Miyoshi N (2000) *Device for purifying exhaust gas from an internal combustion engine*. US Patent, 6119452 (Sept. 19, 2000)
43. Sakurai K (2011) *Exhaust purifying system for internal combustion engine*. US Patent Appl. 2011/0138783 A1 (June 16, 2011)

44. Sakurai K, Miyashita S, Katumata Y (2011) *Exhaust purifying system for internal combustion engine*. US Patent Appl. 2011/0214417 A1 (Sep. 8, 2011)
45. Guenther J, Konrad B, Krutzsch B, Nolte A, Voigtlaender D, Weibel M, Wenninger G (2002) *Exhaust gas purification process and apparatus with internal generation of ammonia for reducing nitrogen oxide*. US Patent 6338244 B1 (Jan. 15, 2002)
46. Gandhi HS, Cavatalo JV, Hammerle RH, Chen Y (2004) *Catalyst system for NOx and NH3 emission*. US Patent Appl. 2004/0076565 A1 (Apr. 22, 2004)
47. Gandhi HS, Cavatalo JV, Hammerle RH, Chen Y (2008) *Catalyst system for NOx and NH3 emission*. US Patent 7332135 (Feb. 19, 2008)
48. Chigapov A., Carberry B, Ukropec R, *LNT and SCR catalysts for combined LNT-SCR applications*. Patent EP 2 481 473 A2 and EP 2 481 473 A3 (26 Jan. 2011)
49. Li Y, Deeba M, Dettling JC (2005) *Emissions treatment system with NSR and SCR catalysts*. Patent WO 2005/047663 A3 (26 May 2005)
50. Furbeck H, Koermer G. S, Moini A, Castellano CR (2008) *Catalyst, method for its prepration and system to reduce NOx in an exhaust gas stream*. Patent WO 2008/036797 A1 (27 March 2008)
51. Wan CZ, Zheng X, Stiebels S, Wendt C, Boorse SR (2010) *Emissions treatment system with ammonia-generating and SCR catalyst*. Patent WO 2010/114873 A3 (7 October 2010)
52. Li Y, Deeba M, Dettling JC, Patchett JA, Roth SA, *Emission treatment system with NSR and SCR catalysts*, Patent US 7919051B2 (5 April 2011)
53. Chen HY, Weigert E, Fedeyko J, Cox J, Andersen P (2010) *Advanced Catalysts for Combined (NAC + SCR) Emission Control Systems*. SAE Technical Paper 2010-01-0302
54. Twigg MV (2011) *Catalytic control of emissions from cars*. Catal. Today 163:33–41
55. Hu H. Stover Th. (2006) *Hybrid catalyst system for exhaust emissions reduction*, Patent WO 2006/008625 A1 (26 Jan. 2006)
56. Hu H. Stover Th. (2007) *Hybrid catalyst system for exhaust emissions reduction*, Patent US 7213395 B2 (8 May 2007)
57. Hu H, Mc Carthy E. Jr, Yan Y (2007) *Thermal management of hybrid LNT/SCR aftertreatment during desulfation*, Patent US 7251929 B2 (7 Aug. 2007)
58. Hu H. Stover Th. (2010) *Hybrid catalyst system for exhaust emissions reduction*, Patent US 7650746 B2 (26 Jan. 2010)
59. Mc Carthy E. Jr, Bailey OH (2011) *LNT-SCR system optimized for thermal gradient*, Patent US 7950226 B2 (31 May 2011)
60. Ginter DM, Mc Carthy E. Jr (2011) *Optimized rhodium usage in LNT-SCR system*, Patent US 8069654 B2 (6 Dec. 2011)
61. T. Nakatsuji, M. Matsubara, J. Rouistenmäki, N. Sato, H. Ohno (2007) *A NOx reduction system using ammonia-storage selective catalytic reduction in rich/lean excursions*, Appl. Catal. B: Environmental 77: 190–201
62. H. Shinjoh, N. Takahashi, K. Yokota (2007) *Synergic effect of Pd/gamma-alumina and Cu/ZSM-5 on the performance of NOx storage reduction catalyst*, Topics Catal., 42-43: 215–219
63. E.C. Corbos, M. Haneda, X. Courtois, P. Marecot, D. Duprez (2008) H. Hamada, *Cooperative effect of Pt–Rh/Ba/Al and CuZSM-5 catalysts for NOx reduction during periodic lean-rich atmosphere*, Catal. Comm., 10: 137–141
64. E.C. Corbos, M. Haneda, X. Courtois, P. Marecot, D. Duprez (2009) H. Hamada, *NOx abatement for lean-burn engines under lean–rich atmosphere over mixed NSR-SCR catalysts: Influences of the addition of a SCR catalyst and of the operational conditions*, Appl. Catal. A: General, 365: 187–193
65. J. Wang, Y. Ji, Z. He, M. Crocker, M. Dearth, R. W. McCabe (2012) *A non-NH3 pathway for NOx conversion in coupled LNT-SCR systems,* Appl. Catal. B: Environmental 111–112: 562–570
66. J. Theis, J. Ura, R. McCabe (2010) *The Effects of Sulfur Poisoning and Desulfation Temperature on the NOx Conversion of LNT+SCR Systems for Diesel Applications*, SAE

Technical Papers, 2010-01-300 & SAE Int. J. Fuels Lubr. 3 (2010) 1–15, doi:10.4271/2010-01-0300
67. L. Xu, R. W. McCabe, *LNT + in situ SCR catalyst system for diesel emissions control*, Catal. Today 184 (2012) 83–94
68. U. De La Torre, B. Pereda-Ayo, J. R. González-Velasco, *Cu-zeolite NH3–SCR catalysts for NOx removal in the combined NSR–SCR technology*, Chem. Eng. J. in press, doi:10.1016/j.cej.2012.06.092
69. Bonzi R, Lietti L, Castoldi L, Forzatti P (2010) *NOx removal over a double-bed NSR-SCR reactor configuration.* Catal. Today 151:376–385
70. Forzatti P, Lietti L (2010) *The reduction of NOx stored on LNT and combined LNT–SCR systems.* Catal. Today 155:131–139
71. Castoldi L, Bonzi R, Lietti L, Forzatti P, Morandi S, Ghiotti G, Dzwigaj S (2011) 45 *Catalytic behaviour of hybrid LNT/SCR systems: Reactivity and in situ FTIR study.* J. Catal. 282:128–144
72. Zukerman R, Vradman L, Herskowitz M, Liverts E, Liverts M, Massner A, Weibel M, Brilhac JF, Blakeman PG, Peace LJ (2009) *Modeling and simulation of a smart catalytic converter combining NOx storage, ammonia production and SCR*. Chem. Eng. J. 155:419–426
73. Weibel M, Waldbüßer N, Wunsch R, Chatterjee D, Bandl-Konrad B, Krutzsch B (2009) *A Novel Approach to Catalysis for NOx Reduction in Diesel Exhaust Gas*. Top. Catal. 52:1702–1708
74. Chatterjee D, Kočí P, Schmeiser V, Marek M, Weibel M (2010) *Modelling of NOx Storage + SCR Exhaust Gas Aftertreatment System with Internal Generation of Ammonia*. SAE Technical Papers, 2010-01-0887
75. Chatterjee D, Kočí P, Schmeiser V, Marek M, Weibel M, Krutzsch B (2010) *Modelling of a combined NOx storage and NH3-SCR catalytic system for Diesel exhaust gas aftertreatment*. Catal. Today 151:395–409
76. Lindholm A, Sjövall H, Olsson L (2010) *Reduction of NOx over a combined NSR and SCR system*. Appl. Catal. B 98:112–121
77. Seo CK, Kim H, Choi B, Lim MT, Lee CH, Lee CB (2011) *De-NOx characteristics of a combined system of LNT and SCR catalysts according to hydrothermal aging and sulfur poisoning*. Catal. Today 164:507–514
78. Pereda-Ayo B, Duraiswami D, González-Velasco JR (2011) *Control of NOx storage and reduction in NSR bed for designing combined NSR–SCR systems*. Catal. Today 172:66–72
79. Liu Y, Harold MP, Luss D (2012) *Coupled NOx storage and reduction and selective catalytic reduction using dual-layer monolithic catalysts*, Appl. Catal. B 121–122:239–251
80. Seo CK, Kim H, Choi B, Lim MT (2011) *The optimal volume of a combined system of LNT and SCR catalysts*. J. Ind. Eng. Chem. 17:382–385
81. Kota AS, Luss D, Balakotaiah V (2012), *Modeling Studies on Lean NOx Reduction by a Sequence of LNT−SCR Bricks*, Ind. Eng. Chem. Res. 51:6686–6696
82. Sullivan JA, Keane O (2007) *A combination of NOx trapping materials and urea-SCR catalysts for use in the removal of NOx from mobile diesel engines*. Appl. Catal. B 70:205–214
83. Can F, Berland S, Royer S, Courtois X, Duprez D. *Composition dependant performance of CexZr1-xO2 mixed-oxide supported WO3 catalysts for the NSR–SCR coupled process.* submitted
84. Berland S (2011) PhD thesis, University of Poitiers. http://www2.ademe.fr/jsp/theses/these.jsp?num=2353&catid=13842
85. Lietti L (1996) *Reactivity of V2O5–WO3/TiO2 de–NOx catalysts by transient methods* Appl. Catal. B 10: 281–297
86. Kim MK, Kim PS, Cho BK, Nam IS, Oh SH (2012) *Enhanced NOx reduction and byproduct removal by (HC + OHC)/SCR over multifunctional dual-bed monolith catalyst*. Catal. Today 184:95–106

87. Brandenberger S, Kröcher O, Tissler A, Althoff R (2008) *The State of the Art in Selective Catalytic Reduction of NOx by Ammonia Using Metal-Exchanged Zeolite Catalysts.* Catal. Rev. 50:492–531
88. Koebel M, Madia G, Elsener M (2002) *Selective catalytic reduction of NO and NO2 at low temperatures.* Catal. Today 73:239–247
89. Nova I, Ciardelli C, Tronconi E, Chatterjee D, Bandl-Konrad B (2006) *NH3–NO/NO2 chemistry over V-based catalysts and its role in the mechanism of the Fast SCR reaction.* Catal. Today 114:3–12
90. Forzatti P, Lietti L, Tronconi E (2002) Nitrogen Oxides Removal—Industrial in: I.T. Horvath (Ed.) Encyclopaedia of Catalysis, first ed., Wiley, New York, and references therein
91. Kato A, Matsuda S, Kamo T, Nakajima F, Kuroda H,.Narita T (1981) *Reaction between nitrogen oxide (NOx) and ammonia on iron oxide-titanium oxide catalyst.* J. Phys. Chem. 85:4099–4102
92. Apostolescu N, Geiger B, Hizbullah K, Jan MT, Kureti S, Reichert D, Schott F, Weisweiler W (2006) *Selective catalytic reduction of nitrogen oxides by ammonia on iron oxide catalysts.* Appl. Catal. B. 62:104–114
93. Luo JY, Hou X, Wijayakoon P, Schmieg SJ, Li W, Epling WS (2011) *Spatially resolving SCR reactions over a Fe/zeolite catalyst.* Appl. Catal. B. 102:110–119
94. Ozkan US, Cai Y, Kumthekar MW (1994) *Investigation of the Reaction Pathways in Selective Catalytic Reduction of NO with NH3 over V2O5 Catalysts: Isotopic Labeling Studies Using 18O2, 15NH3, 15NO, and 15N18O.* J. Catal. 149:390–403
95. Odenbrand CUI, Bahamonde A, Avila P, Blanco J (1994) *Kinetic study of the selective reduction of nitric oxide over vanadia—tungsta—titania/sepiolite catalyst.* Appl. Catal. B. 5:117–131
96. Ramis G, Busca G, Bregani F, Forzatti P (1990) *Fourier transform-infrared study of the adsorption and coadsorption of nitric oxide, nitrogen dioxide and ammonia on vanadia-titania and mechanism of selective catalytic reduction.* Appl. Catal. 64:259–278
97. Kiel JHA, Edelaar ACS, Prins W, van Swaaij WPM (1991) *Performance of silica-supported copper oxide sorbents for SOx/NOx-removal from flue gas: II. Selective catalytic reduction of nitric oxide by ammonia.* Appl. Catal. B. 1:41–60
98. Hsu LY, Teng H (2001) *Catalytic NO reduction with NH3 over carbons modified by acid oxidation and by metal impregnation and its kinetic studies.* Appl. Catal. B. 35:21–30
99. Lobree LJ, Hwang IC, Reimer JA, Bell AT (1999) *Investigations of the State of Fe in H–ZSM-5.* J. Catal. 186:242–253
100. Long RQ, Yang RT (2000) *Characterization of Fe-ZSM-5 Catalyst for Selective Catalytic Reduction of Nitric Oxide by Ammonia*. J. Catal. 194:80–90
101. Wallin M, Karlsson CJ, Skoglundh M, Palmqvist A. (2003) *Selective catalytic reduction of NOx with NH3 over zeolite H–ZSM-5: influence of transient ammonia supply.* J. Catal. 218:354–364
102. Busca G, Larrubia MA, Arrighi L, Ramis G (2005) *Catalytic abatement of NOx: Chemical and mechanistic aspects,* Catal. Today 107–108:139–148
103. Koebel M, Elsener M, Madia G (2001) *Reaction Pathways in the Selective Catalytic Reduction Process with NO and NO2 at Low Temperatures.* Ind. Eng. Chem. Res. 40:52–59
104. Yeom Y, Henao J, Li M,. Sachtler WMH, Weitz E (2005) *The role of NO in the mechanism of NOx reduction with ammonia over a BaNa–Y catalyst.* J. Catal. 231:181–193
105. Ciardelli C, Nova I, Tronconi E, Chatterjee D, Burkhardt T, Weibel M (2007) *NH3 SCR of NOx for diesel exhausts aftertreatment: role of NO2 in catalytic mechanism, unsteady kinetics and monolith converter modelling.* Chem. Eng. Sci. 62:5001–5006
106. Devadas M, Kröcher O, Elsener M, Wokaun A, Söger N, Pfeifer M, Demel Y, Mussmann L (2006) *Influence of NO2 on the selective catalytic reduction of NO with ammonia over Fe-ZSM-5.* Appl. Catal. B. 67:187–196

107. Hadjiivanov K, Knözinger H, Tsyntsarski B, Dimitrov L (1999) *Effect of Water on the Reduction of NOx with Propane on Fe–ZSM-5. An FTIR Mechanistic Study.* Catal. Lett. 62:35–40
108. Lobree LJ, Hwang IC, Reimer JA, Bell AT (1999) *Investigations of the State of Fe in H–ZSM-5.* J. Catal. 186:242–253
109. Veley VH, (1993) *The Conditions of Decomposition of Ammonium Nitrite,* J. Am. Chem. Soc. 83:736–749
110. Romero Sarria F, Saussey J, Gallas JP, Marie O, Daturi M (2005) *In situ and operando IR study of adsorption sites for NH4+ active species in NOx–SCR via NH3 using a Y zeolite.* Stud. Surf. Sc. Catal. 158(A):821–828
111. Grossale A, Nova I, Tronconi E, Chatterjee D, Weibel M (2008) *The chemistry of the NO/NO2–NH3 "fast" SCR reaction over Fe-ZSM-5 investigated by transient reaction analysis.* J. Catal. 256:312–322
112. Wilken N, Wijayanti K, Kamasamudram K, Currier NW, Vedaiyan R, Yezerets A, Olsson L (2012) *Mechanistic investigation of hydrothermal aging of Cu–Beta for ammonia* 48 *SCR,* Appl. Catal. B 111–112:58–66
113. Rahkamaa-Tolonen K, Maunula T, Lomma M, Huuhtanen M, Keiski RL (2005) *The effect of NO2 on the activity of fresh and aged zeolite catalysts in the NH3–SCR reaction.* Catal. Today 100:217–222
114. Tuenter G, Vanleeuwen WF, Snepvangers LJM (1986) *Kinetics and Mechanism of the NOx Reduction with NH3 on V2O5–WO3–TiO2 Catalyst.* Ind. Eng. Chem. Prod. Res. Dev. 25(4):633–636
115. Sun Q, Gao ZX, Chen HY, Sachtler WMH (2001) *Reduction of NOx with Ammonia over Fe/MFI: Reaction Mechanism Based on Isotopic Labeling.* J. Catal. 201:88–99
116. Long RQ, Yang RT (2002) *Reaction Mechanism of Selective Catalytic Reduction of NO with NH3 over Fe–ZSM-5 Catalyst.* J. Catal. 207:224–231
117. Long RQ, Yang RT (2001) *Temperature-Programmed Desorption/Surface Reaction (TPD/TPSR) Study of Fe–Exchanged ZSM-5 for Selective Catalytic Reduction of Nitric Oxide by Ammonia.* J. Catal. 198:20–28
118. Long RQ, Yang RT (1999) *Catalytic Performance of Fe–ZSM-5 Catalysts for Selective Catalytic Reduction of Nitric Oxide by Ammonia.* J. Catal. 188:332–339
119. Eng J, Bartholomew CH (1997) *Kinetic and Mechanistic Study of NOx Reduction by NH3 over H–Form Zeolites. II. Semi-Steady-State and In Situ FTIR Studies.* J. Catal. 171:27–44
120. Stevenson SA, Vartuli JC, Sharma SB (2002) *The Effects of Steaming and Sodium Exchange on the Selective Catalytic Reduction of NO and NO2 by NH3 over HZSM-5.* J. Catal., 208:106–113
121. Armaroli T, Simon LJ, Digne M, Montanari T, Bevilacqua M, Valtchev V, Patarin J, Busca G (2006) *Effects of crystal size and Si/Al ratio on the surface properties of H–ZSM-5 zeolites.* Appl. Catal. A. 306:78–84
122. Brandenberger S, Kröcher O, Wokaun A, Tissler A, Althoff R (2009) *The role of Brønsted acidity in the selective catalytic reduction of NO with ammonia over Fe–ZSM-5.* J. Catal. 268:297–306
123. Schwidder M, Kumar MS, Bentrup U, Pérez-Ramírez J, Brückner A, Grünert W (2008) *The role of Brønsted acidity in the SCR of NO over Fe-MFI catalysts.* Micro. Meso. Mater. 111:124–133
124. Védrine JC, Auroux A, Bolis V, Dejaifve P, Naccache C, Wierzchowski P, Derouane EG, Nagy JB, Gilson JP, van Hooff JHC, van den Berg JP, Wolthuizen J (1979) *Infrared, microcalorimetric, and electron spin resonance investigations of the acidic properties of the H–ZSM-5 zeolite.* J. Catal. 59:248–262
125. Topsøe NY, Pedersen K, Derouane EG (1981) *Infrared and temperature-programmed desorption study of the acidic properties of ZSM-5-type zeolites.* J. Catal. 70:41–52
126. Brüggemann TC, Vlachos DG, Keil FJ (2011) *Microkinetic modeling of the fast selective catalytic reduction of nitrogen oxide with ammonia on H–ZSM-5 based on first principles.* J. Catal. 283:178–191

127. Colombo M, Nova I, Tronconi E (2010) A comparative study of the NH3-SCR reactions over a Cu–zeolite and a Fe–zeolite catalyst. Catal. Today 151: 223–230
128. Kieger S, Delahay G, Coq B, Neveu B (1999) *Selective Catalytic Reduction of Nitric Oxide by Ammonia over Cu–FAU Catalysts in Oxygen-Rich Atmosphere.* J. Catal. 183:267–280
129. Moretti G, Dossi C, Fusi A, Recchia S, Psaro R (1999) *A comparison between Cu-ZSM-5, Cu–S–1 and Cu–mesoporous-silica–alumina as catalysts for NO decomposition*. Appl. Catal. B20:67–73
130. Dossi C, Fusi A, Recchia S, Psaro R, Moretti G (1999) *Cu–ZSM-5 (Si/Al=66), Cu–Fe–S–1 (Si/Fe=66) and Cu–S–1 catalysts for NO decomposition: preparation, analytical characterization and catalytic activity.* Microp. Mesop. Mater. 30:165–175
131. Mizumoto M, Yamazoe N, Seiyama T (1978) *Catalytic reduction of NO with ammonia over Cu(II) NaY.* J. Catal. 55:119–128
132. Iwamoto M, Yahiro H, Tanda K, Mizuno N, Mine Y, Kagawa S (1991) *Removal of Nitrogen Monoxide through a Novel Catalytic Process. 1. Decomposition on Excessively Copper–Ion Exchanged ZSM-5 Zeolites.* J. Phys. Chem. 95(9):3727–3730
133. Sjövall H, Olsson L, Fridell E, Blint R.J (2006) Selective catalytic reduction of NOx with NH3 over Cu–ZSM-5—The effect of changing the gas composition. Appl. Catal. B. 64:180–188
134. SeO C-K, Choi B, Kim H, Lee C-H, Lee C-B (2012) *Effect of ZrO2 addition on de–NOx performance of Cu–ZSM-5 for SCR catalyst.* Chem Eng. J. 191:331–340
135. Kwak J.H, Tran D, Burton S.D, Szanyi J, Lee J-H, Peden C (2012) *Effects of hydrothermal aging on NH3–SCR reaction over Cu/zeolites*, J. Catal 287:203–209
136. Marturano P, Drozdová L, Kogelbauer A, Prins R (2000) *Fe/ZSM-5 Prepared by Sublimation of FeCl3: The Structure of the Fe Species as Determined by IR, 27Al MAS NMR, and EXAFS Spectroscopy.* J. Catal. 192:236–247
137. Battiston AA, Bitter JH, de Groot FMF, Overweg AR, Stephan O, van Bokhoven JA, Kooyman PJ, van der Spek C, Vankó G, Koningsberger DC (2003) *Evolution of Fe species during the synthesis of over-exchanged Fe/ZSM-5 obtained by chemical vapor deposition of FeCl3.* J. Catal. 213:251–271
138. Hensen EJM, Zhu Q, Hendrix MMRM, Overweg AR, Kooyman PJ, Sychev MV, van Santen RA (2004) *Effect of high-temperature treatment on Fe/ZSM-5 prepared by chemical vapor deposition of FeCl3: I. Physicochemical characterization.* J. Catal. 221:560–574
139. Joyner R, Stockenhuber M (1999) *Preparation, Characterization, and Performance of Fe−ZSM-5 Catalysts.* J. Phys. Chem. B 103:5963–5976 50
140. Sobalik Z, Vondrova A, Tvaruskova Z, Wichterlova B (2002) *Analysis of the structural parameters controlling the temperature window of the process of SCR–NOx by low paraffins over metal-exchanged zeolites*. Catal. Today 75:347–351
141. Heinrich F, Schmidt C, Löffler E, Grünert W (2000) *A highly active intra-zeolite iron site for the selective catalytic reduction of NO by isobutane*. Catal. Commun. 2:317–321
142. Chen HY, El-Malki M, Wang X, van Santen RA, Sachtler WMH (2000) *Identification of active sites and adsorption complexes in Fe/MFI catalysts for NOx reduction.* J. Mol. Catal. A: Chem. 162:159–174
143. Brandenberger S, Kröcher O, Tissler A, Althoff R (2010) *The determination of the activities of different iron species in Fe–ZSM-5 for SCR of NO by NH3* Appl. Catal. B; 95: 348–357
144. Malpartida I, Marie O, Bazin P, Daturi M, Jeandel X (2012) *The NO/NOx ratio effect on the NH3-SCR efficiency of a commercial automotive Fe–zeolite catalyst studied by operando IR-MS.* Appl. Catal. B. 113–114:52–60
145. Roy S, Viswanath B, Hegde MS, Madras G (2008) *Low-Temperature Selective Catalytic Reduction of NO with NH3 over Ti0.9M0.1O2-δ (M = Cr, Mn, Fe, Co, Cu).* J. Phys. Chem. C. 112:6002–6012
146. Verdier S, Rohart E, Bradshaw H, Harris D et al. (2008) *Acidic Zirconia Materials for Durable NH3–SCR deNOx Catalysts.* SAE Technical Paper 2008-01-1022
147. Rohart E, Kröcher O, Casapu M, Marques R, Harris D, Jones C (2011) *Acidic Zirconia Mixed Oxides for NH_3–SCR Catalysts for PC and HD Applications*. SAE Technical Paper 2011-01-1327